

# Discovery of *N*-(4-Fluoro-3-methoxybenzyl)-6-(2-(((2*S*,5*R*)-5-(hydroxymethyl)-1,4-dioxan-2-yl)methyl)-2*H*-tetrazol-5-yl)-2-methylpyrimidine-4-carboxamide. A Highly Selective and Orally Bioavailable Matrix Metalloproteinase-13 Inhibitor for the Potential Treatment of Osteoarthritis

Peter G. Ruminski,<sup>†</sup> Mark Massa,<sup>†</sup> Joseph Strohbach,<sup>†</sup> Cathleen E. Hanau,<sup>†</sup> Michelle Schmidt,<sup>†</sup> Jeffrey A. Scholten,<sup>†</sup> Theresa R. Fletcher,<sup>†</sup> Bruce C. Hamper,<sup>†</sup> Jeffery N. Carroll,<sup>†</sup> Huey S. Shieh,<sup>†</sup> Nicole Caspers,<sup>†</sup> Brandon Collins,<sup>†</sup> Margaret Grapperhaus,<sup>†</sup> Katherine E. Palmquist,<sup>†</sup> Joe Collins,<sup>†</sup> John E. Baldus,<sup>†</sup> Jeffrey Hitchcock,<sup>†</sup> H. Peter Kleine,<sup>†</sup> Michael D. Rogers,<sup>†</sup> Joseph McDonald,<sup>†</sup> Grace E. Munie,<sup>‡</sup> Dean M. Messing,<sup>§</sup> Silvia Portolan,<sup>§</sup> Laurence O. Whiteley,<sup>||</sup> Teresa Sunyer,<sup>‡</sup> and Mark E. Schnute<sup>\*,†</sup>

<sup>†</sup>Worldwide Medicinal Chemistry and <sup>‡</sup>Inflammation and Immunology Research, Pfizer, 610 Main Street, Cambridge, Massachusetts 02139, United States

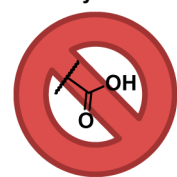
<sup>§</sup>Pharmacokinetics, Dynamics, and Metabolism, Pfizer, 700 North Main Street, Cambridge, Massachusetts 02139, United States

<sup>||</sup>Drug Safety, Pfizer, 1 Burt Road, Andover, Massachusetts 01810, United States

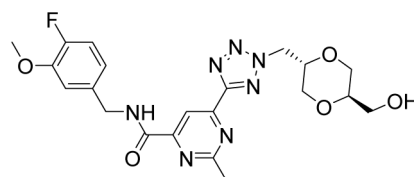
## **S** Supporting Information

**ABSTRACT:** Matrix metalloproteinase-13 (MMP-13) is a zinc-dependent protease responsible for the cleavage of type II collagen, the major structural protein of articular cartilage. Degradation of this cartilage matrix leads to the development of osteoarthritis. We previously have described highly potent and selective carboxylic acid containing MMP-13 inhibitors; however, nephrotoxicity in preclinical toxicology species precluded development. The accumulation of compound in the kidneys mediated by human organic anion transporter 3 (hOAT3) was hypothesized as a contributing factor for the finding. Herein we report our efforts to optimize the MMP-13 leads resulting in the identification of compound 43a lacking

### Carboxylic Acids



hOAT3 Transporter Substrates



43a (MMP-13  $K_i$  = 1.5 nM)

potency and pharmacokinetic properties of non-carboxylic acid leads resulting in the identification of compound 43a lacking the previously observed preclinical toxicology at comparable exposures.

## INTRODUCTION

Osteoarthritis (OA) is a highly debilitating disease characterized by the degeneration of synovial joints especially of the hand, knee, hip, and spine leading to pain and reduced mobility. Based on 2005 data, an estimated 27 million people in the US suffer from OA.<sup>1</sup> As the proportion of elderly in the population and obesity rates are increasing, both risk factors for disease,<sup>2</sup> the incidence of OA disease is expected to continue to rise. At this time, available treatment strategies have been limited to symptomatic pain relief; however, many of these agents have undesired side effects, and they do not address the cause of the disease.<sup>3</sup> The goal of developing a disease modifying osteoarthritis drug (DMOAD) able to halt disease progression has been elusive. However, continued understanding of the underlying biology and advances in clinical trial design are offering new opportunities for potential treatment options.<sup>4</sup>

A hallmark of OA disease onset is the degradation of articular cartilage, and therefore the prevention of this process is a promising strategy to limit the progression of disease. The major structural protein of articular cartilage is type II collagen. Matrix metalloproteinase-13 (MMP-13), a member of a family of zinc-dependent proteases, shows a high specificity for the cleavage of type II collagen. In preclinical models of OA disease, transgenic mice lacking MMP-13 as well as MMP-13 inhibitors have shown reduced cartilage damage compared with control animals.<sup>5–7</sup>

Several broad spectrum metalloproteinase inhibitors have been investigated in human clinical trials; however, a tendinitis-like stiffening of the joints referred to as muscular skeletal syndrome (MSS) has limited development.<sup>8</sup> The lack of this finding in the phenotype of the MMP-13 null mouse as well as

Received: September 15, 2015

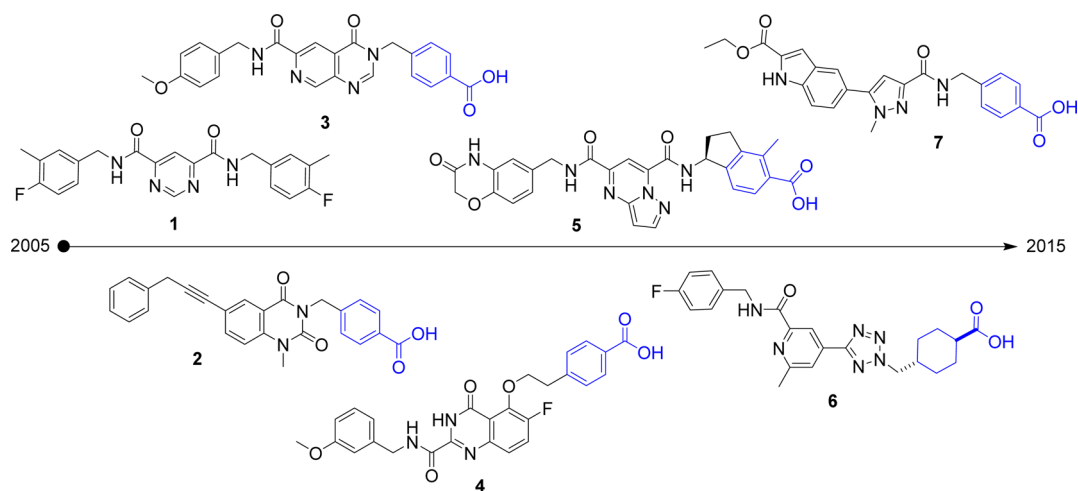


**Figure 1.** Representative non-zinc binding, highly selective MMP-13 inhibitors.

individuals possessing a missense mutation of the MMP-13 gene has suggested the poor selectivity profile of the agents studied was a factor leading to MSS development.<sup>9,10</sup>

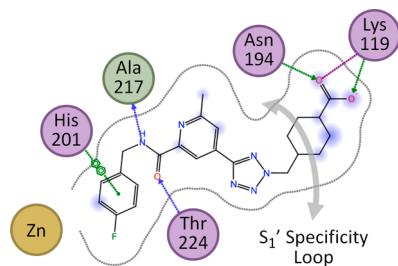
Significant progress in the design of MMP-13 selective inhibitors has occurred over the last 15 years such that several highly selective compounds have been reported in the literature, **Figure 1**. The first reports of MMP-13 specific inhibitors included compound **1** from workers at Aventis<sup>11</sup> and compound **2** from workers at Pfizer.<sup>6</sup> Both compounds were very potent inhibitors of MMP-13 ( $IC_{50}$  = 8 and 0.67 nM, respectively) while showing greater than 10 000-fold selectivity against a panel of related MMP enzymes. Compound **2** was reported to significantly reduce cartilage lesion areas when dosed orally in a rabbit anterior cruciate ligament transection/partial meniscectomy model while not showing MMS-like fibroplasia in rats.<sup>6</sup> The high selectivity was hypothesized to arise by the compound adopting a non-zinc binding mode with the inhibitor occupying a deep region of the  $S_1'$  binding pocket unique to MMP-13. Additional reports of selective MMP-13 inhibitors have appeared from Pfizer (**3** and **6**), Takeda (**4**), Alantos Pharmaceuticals (**5**), and Boehringer Ingelheim (**7**), **Figure 1**.<sup>12–17</sup> The evolution of highly selective MMP-13 inhibitors has led to several core structures; however, with the exception of compound **1**, a terminal carboxylic acid has been maintained as a design element. The preference for the acidic substituent is understandable due to its proximity to Lys-119 in the binding pocket and the potential to form an energetically favorable hydrogen-bond or salt bridge, **Figure 2**.<sup>13,14</sup> Additional important protein–ligand contacts observed for compound **6** include hydrogen bond

contacts between the amide and two residues, Ala-217 and Thr-224, as well as a  $\pi$ – $\pi$  interaction between His-201 and the benzyl ring.

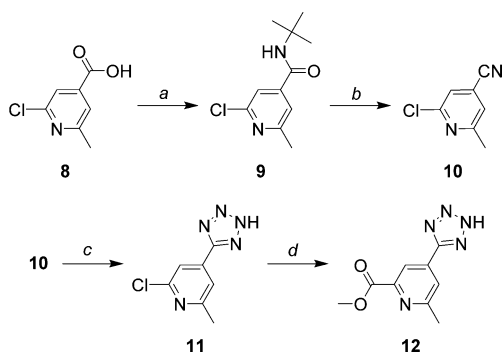
As described in our previous reports, compounds **2**, **3**, and **6** were highly potent and selective MMP-13 inhibitors that demonstrated promising *in vivo* cartilage protection and safety in preclinical rodent studies.<sup>6,12,13</sup> Further studies of all three inhibitors in cynomolgus monkeys however revealed the consistent observation of nephrotoxicity characterized by diffuse tubular epithelial cell degeneration–regeneration.<sup>18</sup> Since these compounds are organic anions, their ability to be transported by human organic anion transporter 1 and 3 (hOAT1/3) was evaluated.<sup>18</sup> Indeed compounds **2**, **3**, and **6** inhibited the uptake of hOAT3 radiolabeled substrate in transfected cell lines ( $IC_{50}$  = 18, 59, and 6  $\mu$ M, respectively) and were found to be accumulated in cultured proximal tubular cells. These results suggested that all three compounds are substrates for the hOAT3 transporter. Carboxylic acids also present the risk of generating reactive metabolites through protein conjugation of the resulting acyl glucuronide.<sup>19</sup> It was hypothesized that the nephrotoxicity finding observed was the consequence of compound accumulation in the kidney epithelial cells followed by a cytotoxic event mediated through the acyl glucuronide metabolite. Compound **6** was specifically selected for its reduced propensity to undergo glucuronide acyl migration to form the reactive species (rearrangement  $T_{1/2}$  = 67 h compared with  $T_{1/2}$  = 0.5 h for diclofenac). Unfortunately, nephrotoxicity was still observed. As a result, a chemistry strategy was undertaken to identify a potent and highly selective MMP-13 inhibitor based on **6** lacking an organic anion functionality to mitigate the transporter mediated accumulation risk.

## CHEMISTRY

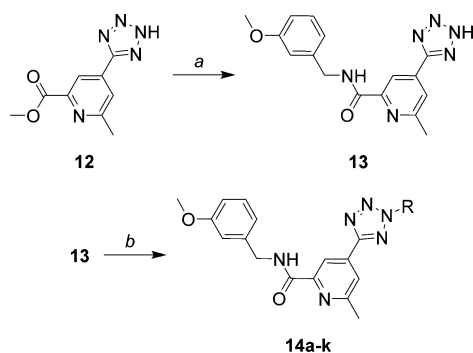
Pyridine tetrazole **12** was utilized as a versatile intermediate allowing for diversity exploration to either the left- or right-hand side of the molecules, **Scheme 1**. Compound **12** was prepared from pyridine carboxylic acid **8** by first transformation of the carboxylic acid to the nitrile via dehydration of the *tert*-butylamide **9**. Sodium azide addition to cyanopyridine **10** afforded tetrazole **11**, which was subjected to palladium-mediated carbonylation to provide ester **12**. In order to facilitate a systematic survey of substituents to the tetrazole, ester **12** was condensed with 3-methoxybenzylamine to provide amide **13**, **Scheme 2**. Alkylation of the tetrazole occurred with high



**Figure 2.** Key protein–ligand interactions between MMP-13 and compound **6**.<sup>13</sup> Blue shading indicates ligand exposed regions; purple indicates polar residues; green indicates hydrophobic residues.

Scheme 1. Synthesis of Pyridine Tetrazole 12<sup>4a</sup>

<sup>4a</sup>Reagents and conditions: (a) oxalyl chloride, DMF, CH<sub>2</sub>Cl<sub>2</sub>; *t*-butylamine; (b) POCl<sub>3</sub>, toluene, 110 °C; (c) Et<sub>3</sub>N·HCl, NaN<sub>3</sub>, toluene, 110 °C; (d) Et<sub>3</sub>N, dppf, Pd(OAc)<sub>2</sub>, MeOH, CO, 100 °C.

Scheme 2. General Synthesis of 14a–k<sup>4a</sup>

<sup>4a</sup>Reagents and conditions: (a) 3-methoxybenzylamine, 100 °C; (b) PS–PPh<sub>3</sub>, DBAD, ROH, THF; or in the case of 14e and 14i, ROSO<sub>2</sub>Y (Y = 4-toluenyl, 4-nitrophenyl), Et<sub>3</sub>N, DMA, 85 °C.

regioselectivity at the 2-position to provide analogs such as 14a–k (Table 1) employing the reaction with alcohols under Mitsunobu conditions or with arylsulfonate esters in the case of 14e and 14i. Additional examples of 4-substituted methylenecyclohexane analogs were prepared as described in Schemes 3–5. Compound 13 was alkylated by methyl *trans*-4-(hydroxymethyl)cyclohexane carboxylate using Mitsunobu conditions to provide ester 17. The resulting ester was then converted to the primary amide 18 and subsequently through dehydration to the nitrile 19. Similarly, 4-amino-substituted analogs were prepared by alkylation of 13 with *trans*- or *cis*-alcohols 20 and 24 using Mitsunobu conditions, Schemes 4 and 5. Subsequent deprotection afforded the corresponding amines (22 and 26), which through either acylation or sulfonylation provided *trans*-isomers 23a,b and *cis*-isomers 27a,b. Piperidine analogs were also prepared through Mitsunobu alkylation of 13 with alcohol 28, Scheme 6. Deprotection of the resulting product (29) followed by acylation or sulfonylation provided piperidine amide 31a or sulfonamide 31b.

In order to survey substitution to the benzylamide, carboxylic acid 33 was employed as the common intermediate, Scheme 7. Compound 13 was alkylated with *trans*-cyclohexane-1,4-dimethanol using Mitsunobu conditions to provide ester 32, which was subsequently saponified to provide acid 33. Amide analogs 34a–k (Table 2) were then prepared by coupling of the corresponding substituted benzylamine with compound 33.

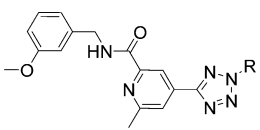
The synthesis of pyrimidine tetrazole analogs followed a similar synthetic sequence to that of the pyridine series

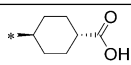
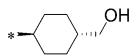
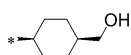
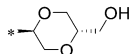
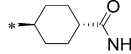
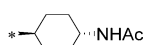
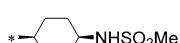
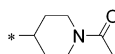
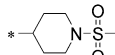
employing cyanopyrimidine 35 as a key intermediate, Scheme 8. Dichloropyrimidine 35 was hydrolyzed under acidic conditions to afford compound 36. The resulting desymmetrization allowed for the effective monocarbonylation of compound 35 through the sequence of palladium mediated carbonylation resulting in compound 37 followed by chlorination yielding ester 38. Tetraethylammonium cyanide was found to efficiently effect displacement of the chloride to provide cyanopyrimidine 39. Condensation of compound 39 with either 3-methoxybenzylamine or 4-fluoro-3-methoxybenzylamine afforded amides 40a and 40b, respectively, Scheme 9. Tetrazoles 41a and 41b were provided by heating a water suspension of the nitriles with sodium azide and zinc bromide. In contrast to the pyridine tetrazole series where alkylation was regioselective at the 2-position, alkylation of 41a,b by tosylate 16 derived from *trans*-2,5-bis(hydroxymethyl)-1,4-dioxane<sup>20</sup> resulted in a mixture of regioisomers (1/1, N2-desired/N1). The pure 2-substituted tetrazoles 42 or 43a,b could be obtained after chromatographic separation. It was subsequently found that the use of metal additives could alter the alkylation regioisomeric ratio to favor the 2-position presumably through chelate formation with the pyrimidine nitrogen. The best selectivity obtained was 5/1 (N2-desired/N1) employing Co(acac)<sub>2</sub> in DMA. The absolute stereochemistry of compounds 43a,b (and by inference tosylate 16) was established by single crystal X-ray analysis of the bromomethyldioxane 44 (Supporting Information) obtained by halogenation of 43a with polymer-supported triphenylphosphine and carbon tetrabromide. Oxidation of 43a by pyridinium dichromate afforded the corresponding carboxylic acid 45.

## RESULTS AND DISCUSSION

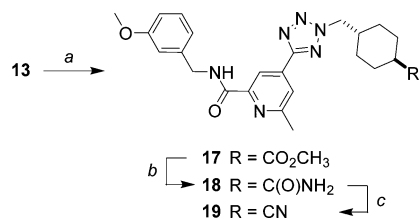
The carboxylic acid functionality in compound 6 had been found to impart favorable properties in previous MMP-13 inhibitor SAR studies including good potency, high metabolic stability, and excellent oral bioavailability. We anticipated several challenges by departing from the carboxylic acid in order to test the transporter-driven toxicology hypothesis. The carboxylic acid provided excellent potency through interactions with Lys-119; therefore an appropriate surrogate would need to be identified or potency enhancement elsewhere in the molecule utilized. Also, carboxylic acid based analog 6 demonstrated high metabolic stability with low clearance and excellent oral bioavailability in rat ( $F = 100\%$ ,  $CL = 14 \text{ mL min}^{-1} \text{ kg}^{-1}$ ). Due to the relatively high lipophilicity of the scaffold in the absence of the acid ( $c\text{LogP} = 5.2$ ), metabolic stability concerns were anticipated. Lastly, the potential for low aqueous solubility of a non-carboxylic acid series was another design concern since salt formation by the core scaffold would be more limited.

Initial efforts focused on the identification of an appropriate replacement for the cyclohexane carboxylic acid motif found in 6, which maintained MMP-13 potency and selectivity, Table 1. For the tetrazole substituent, the structural motif of a methylene linker to a six-membered ring was desired to be maintained due to the importance of this substituent to be accommodated in the tunnel region beneath the MMP-13 S<sub>1</sub>' loop region, Figure 2. For this initial survey, we also chose the 3-methoxybenzylamide for the left-hand substituent as this was one of the most potent substitution patterns in the previous carboxylic acid series (14a, MMP-13  $K_i = 0.16 \text{ nM}$ ).<sup>6</sup> As anticipated, truncation of the carboxylic acid to afford the unsubstituted cyclohexyl analog 14b resulted in a significant but potentially optimizable loss of potency ( $K_i = 33.6 \text{ nM}$ ). We were further pleased to see that oxygen heterocycles including tetrahydropyrans (14c–e) and

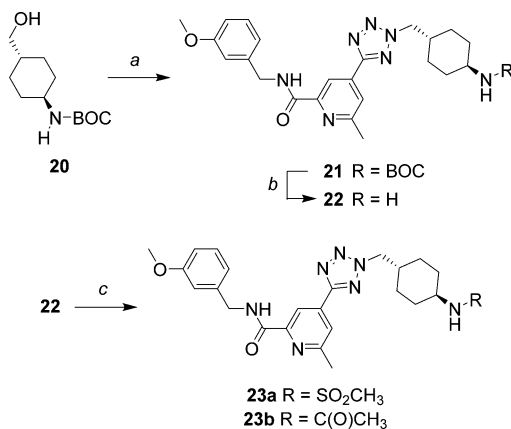
Table 1. SAR of Non-carboxylic Acid Substituents<sup>a</sup>


R	Compound	Config	MMP-13/FL K <sub>i</sub> (nM)	MMP-3/CD K <sub>i</sub> (nM)
	<b>14a</b>		0.16	>10,000
	<b>14b</b>		33.6	>10,000
	<b>14c</b>	(-)	7.7	ND
	<b>14d</b>	(+)	16.8	>10,000
	<b>14e</b>	rac	16.5	>10,000
	<b>14f</b>	rac	14.1	>10,000
	<b>14g</b>		2.1	>10,000
	<b>14h</b>		4.1	8,730
	<b>14i</b>	rac	11.7	>10,000
	<b>14j</b>		4.5	>10,000
	<b>14k</b>		10.9	>10,000
	<b>18</b>		21.2	ND
	<b>19</b>		2.7	7,210
	<b>23a</b>		0.25	>10,000
	<b>23b</b>		2.0	>10,000
	<b>27a</b>		8.2	>10,000
	<b>27b</b>		1.4	>10,000
	<b>31a</b>		16.6	>10,000
	<b>31b</b>		5.8	>10,000

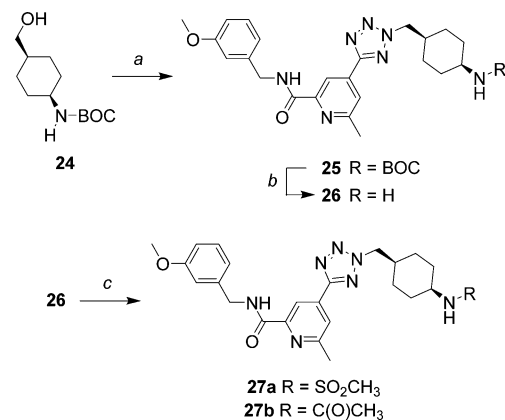
<sup>a</sup>All values are the mean of two or more independent assays. ND, not determined.

Scheme 3. Synthesis of 18 and 19<sup>a</sup>

<sup>a</sup>Reagents and conditions: (a) PS-PPh<sub>3</sub>, DBAD, methyl *trans*-4-(hydroxymethyl)cyclohexanecarboxylate, THF; (b) HCONH<sub>2</sub>, THF, 80 °C, NaOMe; (c) PS-PPh<sub>3</sub>, CCl<sub>4</sub>, DCE, 80 °C.

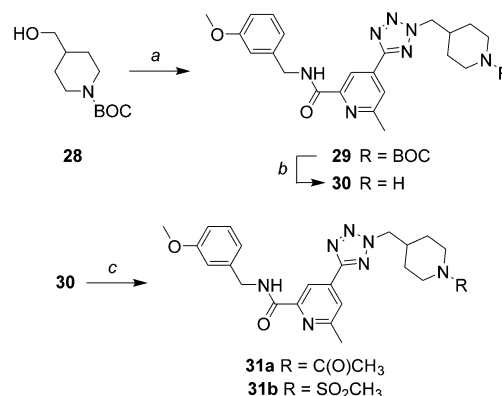
Scheme 4. Synthesis of 23<sup>a</sup>

<sup>a</sup>Reagents and conditions: (a) PS-PPh<sub>3</sub>, DBAD, 13, THF; (b) TFA, CH<sub>2</sub>Cl<sub>2</sub>; (c) Et<sub>3</sub>N, CH<sub>3</sub>SO<sub>2</sub>Cl or Ac<sub>2</sub>O, silica-bound DMAP, CH<sub>2</sub>Cl<sub>2</sub>.

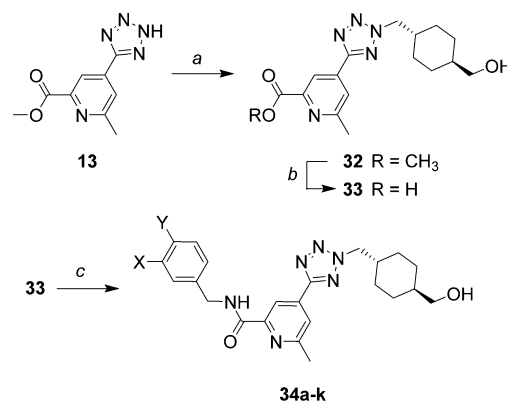
Scheme 5. Synthesis of 27<sup>a</sup>

<sup>a</sup>Reagents and conditions: (a) PS-PPh<sub>3</sub>, DBAD, 13, THF; (b) TFA, CH<sub>2</sub>Cl<sub>2</sub>; (c) Et<sub>3</sub>N, CH<sub>3</sub>SO<sub>2</sub>Cl or Ac<sub>2</sub>O, silica-bound DMAP, CH<sub>2</sub>Cl<sub>2</sub>.

the dioxane (14f) offered comparable potency to the cyclohexane ring and allowed for a potential strategy to reduce the lipophilicity of this group (*vide infra*). Substitution of the cyclohexane ring at the 4-position by either hydroxymethyl (14g,h) or hydroxyl (14j) provided a significant improvement in potency consistent with the potential for hydrogen bond interactions with Lys-119 or Asn-194. Transformation of the carboxylic acid to the primary carboxamide 18 again resulted in significant loss of potency, while the nitrile 19 allowed for a partial recovery of potency similar to that observed with hydroxymethyl substitution (14g). *N*-Acyl and sulfonyl deriva-

Scheme 6. Synthesis of 31<sup>a</sup>

<sup>a</sup>Reagents and conditions: (a) PS-PPh<sub>3</sub>, DBAD, 13, THF; (b) TFA, CH<sub>2</sub>Cl<sub>2</sub>; (c) Et<sub>3</sub>N, silica-bound DMAP, CH<sub>2</sub>Cl<sub>2</sub>; CH<sub>3</sub>SO<sub>2</sub>Cl or Ac<sub>2</sub>O.

Scheme 7. General Synthesis of 34a-k<sup>a</sup>

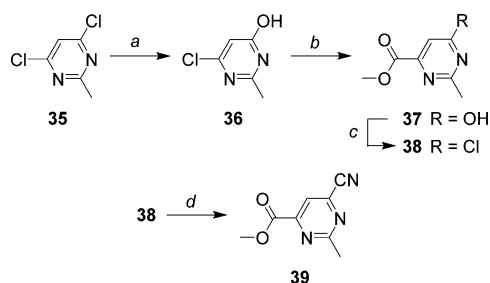
<sup>a</sup>Reagents and conditions: (a) PS-PPh<sub>3</sub>, DBAD, *trans*-cyclohexane-1,4-dimethanol, THF; (b) LiOH, THF, water; (c) 1-hydroxybenzotriazole, DMF, *N*-methylmorpholine, EDCl, corresponding benzylamine.

Table 2. SAR of Benzylamide Substituent<sup>a</sup>

compound	X	Y	MMP-13/FL K <sub>i</sub> (nM)	CYP2C9 inh (%) <sup>b</sup>
34a	H	H	119	78
34b	H	F	32.9	56
34c	F	H	110	<sup>c</sup>
34d	Cl	H	38.5	<sup>c</sup>
34e	CH <sub>3</sub>	H	47.2	93
34f	CF <sub>3</sub>	H	23.8	94
14g	OCH <sub>3</sub>	H	2.1	66
34g	F	F	29.3	83
34h	Cl	F	4.0	90
34i	CH <sub>3</sub>	F	3.8	96
34j	CF <sub>3</sub>	F	6.3	90
34k	OCH <sub>3</sub>	F	1.2	39

<sup>a</sup>All values are the mean of two or more independent assays.

<sup>b</sup>Inhibition of the metabolism of probe substrate diclofenac (5 μM) at an inhibitor test concentration of 3 μM after 8 min incubation with pooled HLM. <sup>c</sup>Not determined.

Scheme 8. Synthesis of Cyanopyrimidine 39<sup>a</sup>

<sup>a</sup>Reagents and conditions: (a) 13 M H<sub>2</sub>SO<sub>4</sub>, rt; (b) Pd(dppf)Cl<sub>2</sub>, iPr<sub>2</sub>EtN, MeOH, CO, 85 °C; (c) oxalyl chloride, DMA, CH<sub>2</sub>Cl<sub>2</sub>, reflux; (d) Et<sub>3</sub>N(CN), DABCO, CH<sub>2</sub>Cl<sub>2</sub>.

tives of 4-amino substituted cyclohexane (23a,b, 27a,b) also showed good potency with the sulfonamide *trans*-isomer 23a achieving MMP-13 potencies comparable to that achieved with a carboxylic acid ( $K_i = 0.25$  nM). Moving the nitrogen atom into the ring as acetyl- (31a) and methylsulfonylpiperidines (31b) was not as favorable.

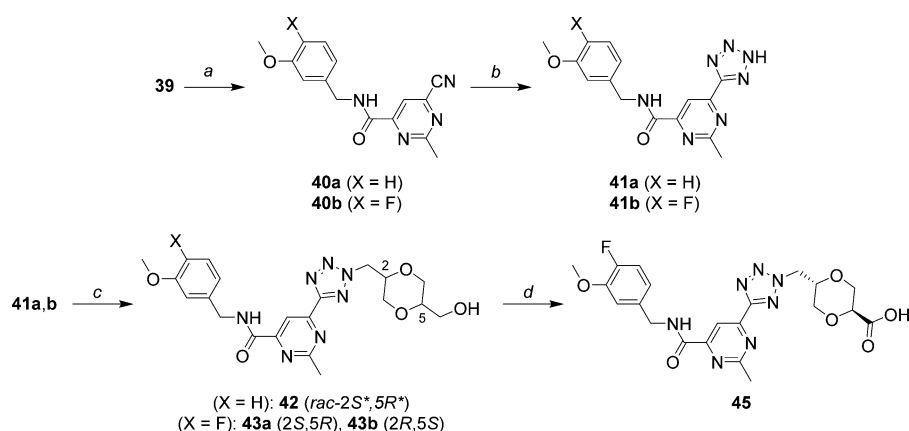
The preferred substitution pattern of the benzylamide group was next re-examined using the *trans*-hydroxymethylcyclohexane analog 14g as a base example, Table 2. A methoxy group at the 3-position of the phenyl ring was clearly favored in the case of monosubstituted analogs (14g, 34a–f). The replacement of hydrogen by fluorine at the 4-position of the phenyl ring (34g–k) consistently improved the potency compared with the monosubstituted analogs with 3-methoxy derivative 34k being the most potent. Several benzyl substitution patterns however were found to present elevated risk of CYP2C9 inhibition, Table 2. Consequently, from this survey 3-methoxybenzyl and 4-fluoro-3-methoxybenzyl were identified as having the best combination of potency and reduced drug–drug interaction liability.

As earlier feared, profiling of select cyclohexyl-based leads for metabolic stability and rat in vivo clearance confirmed that achieving acceptable pharmacokinetics in the non-carboxylic acid series would be a hurdle, Table 3. Compounds 14g, 23a, and 23b each showed moderate to low in vitro intrinsic clearance in human liver microsomes (HLM); however, in vivo clearance after intravenous administration to rats was unacceptably high. In the case of 14g, a higher clearance in rat liver microsomes (RLM)

than in human was consistent with the in vivo observation, and as a result a closer inspection of compounds in assays for both species was warranted. Although amide and sulfonamide derivatives 23a,b avoid the potential direct glucuronide elimination pathway possible with 14g, the modest cLogP reduction ( $\Delta$ cLogP = 0.7–0.9) predicted by modifying the terminal substituent was not sufficient to impact clearance. In order to further reduce the lipophilicity we needed to turn our attention to the cyclohexyl ring.

Metabolic liability of cyclohexane-containing compounds is commonly encountered due to the high relative lipophilicity/atom count of the cyclohexane ring and the susceptibility of all six carbon atoms to oxidative metabolism; therefore, a common strategy has been to replace the cyclohexyl ring with oxygen containing isosters.<sup>22</sup> Guided by the predicted cLogP, the replacement of either one or two cyclohexane carbon atoms with oxygen afforded compounds with lower measured lipophilicity as in the case of tetrahydropyran 14c ( $\Delta$ LogD = –1.15) and dioxane 14f ( $\Delta$ LogD = –1.88). Although compound 14c still showed high clearance, results for dioxane 14f were promising, Table 3. Compound 14f had low clearance in human liver microsomes and even though rat liver microsomal clearance remained high, it showed the lowest rat in vivo clearance to date in the series. Saturated heterocycles are common elements in medicinal chemistry with nitrogen heterocycles being ubiquitous and oxygen heterocycles such as oxetanes and tetrahydropyrans finding growing utility.<sup>23,24</sup> The dioxane ring however has not been widely utilized in drug design.<sup>25–27</sup> Nonetheless, encouraged by the trend, we next combined the dioxane ring with a hydroxymethyl substituent (14i) to further reduce the lipophilicity (LogD = 2.04) and block the potentially metabolically labile carbon on the dioxane ring. Compound 14i maintained good MMP-13 potency ( $K_i = 11.7$  nM) and now achieved low clearance in human and rat liver microsomes. Likewise, 14i demonstrated low rat in vivo clearance (7.7 mL min<sup>–1</sup> kg<sup>–1</sup>) after intravenous injection and good oral bioavailability ( $F = 48\%$ ). Even though the primary metabolic pathway in rat hepatocytes was found to be similar for 14g and 14i, *O*-glucuronidation and hydroxymethyl oxidation, the proximity of the dioxane ring to the hydroxymethyl moiety has a remarkable suppressive effect on the overall metabolism.

To further reduce the lipophilicity, we also considered the transformation of the pyridine core to a pyrimidine (predicted

Scheme 9. Synthesis of 42, 43, and 45<sup>a</sup>

<sup>a</sup>Reagents and conditions: (a) corresponding benzylamine, iPr<sub>2</sub>EtN, MeOH, 35 °C; (b) NaN<sub>3</sub>, ZnBr<sub>2</sub>, water, reflux; (c) 16, Et<sub>3</sub>N, DMA, 85 °C; (d) 43a, pyridinium dichromate, DMF, rt.

**Table 3. In Vitro and Rat In Vivo Pharmacokinetic Data for Select Pyridine Tetrazoles<sup>a</sup>**

compound	cLogP <sup>b</sup>	LogD <sup>c</sup>	HLM <sup>d</sup> ( $\mu\text{L min}^{-1} \text{mg}^{-1}$ )	RLM <sup>d</sup> ( $\mu\text{L min}^{-1} \text{mg}^{-1}$ )	rat CL ( $\text{mL min}^{-1} \text{kg}^{-1}$ )
14b	5.03	4.37	41.7	98.5	63.5 <sup>e</sup>
14c	3.14	3.22	53.1	192	54.5 <sup>e</sup>
14f	1.80	2.49	<8.0	74.0	25.8 <sup>e</sup>
14g	3.56	3.57	32.7	94.9	76.6 <sup>e</sup>
14i	1.11	2.04	<8.0	15.7	7.7 <sup>e</sup>
23a	2.63	<i>f</i>	<8.0	<i>f</i>	42.6 <sup>g</sup>
23b	2.84	<i>f</i>	24.7	<i>f</i>	77.6 <sup>g</sup>

<sup>a</sup>All in vitro values are the mean of two or more independent assays. <sup>b</sup>Calculated LogP using ACD version 12. <sup>c</sup>Measured pH 7.4 LogD by shake-flask method. <sup>d</sup>HLM or RLM in vitro intrinsic CL calculated from metabolic stability data as described in ref 21. <sup>e</sup>Intravenous bolus administration of 1.0 mg/kg ( $N = 2$ ). <sup>f</sup>Not determined. <sup>g</sup>Intravenous bolus administration of 0.2 mg/kg in cassette PK format (5 compounds,  $N = 2$ ).

**Table 4. In Vitro ADME Property Comparison of Pyridine 14i and Pyrimidine 42<sup>a</sup>**

compound	LogD <sup>b</sup>	MMP-13/FL $K_i$ (nM)	MMP-3/CD $K_i$ (nM)	HLM <sup>c</sup> ( $\mu\text{L min}^{-1} \text{mg}^{-1}$ )	sol <sup>d</sup> ( $\mu\text{M}$ )	hPPB (%)
14i	2.04	11.7	>10000	<8.0	28	86
42	1.30	5.8	>10000	<8.0	237	69

<sup>a</sup>All values are the mean of two or more independent assays. <sup>b</sup>Measured pH 7.4 LogD by shake-flask method. <sup>c</sup>HLM in vitro intrinsic CL calculated from metabolic stability data as described in ref 21. <sup>d</sup>Thermodynamic solubility of crystalline solid in pH 7.4 phosphate buffer.

$\Delta\text{cLogP} = -0.58$ ). Compound **42** was prepared to enable direct comparison with pyridine analog **14i**, Table 4. Indeed as predicted, pyrimidine **42** demonstrated a lower measured lipophilicity compared with the pyridine ( $\Delta\text{LogD} = -0.74$ ). The pyrimidine analog also maintained good MMP-13 potency ( $K_i = 5.8$  nM) and high selectivity against MMP-3. While clearance in human liver microsomes remained low for **42**, other pharmaceutical properties were improved compared with the pyridine analog. Compared with pyridine **14i**, aqueous solubility of pyrimidine **42** was improved by more than 8-fold (237 vs 28  $\mu\text{M}$ ) and human plasma protein binding was also reduced (69% vs 86%). Rat pharmacokinetics for **42** was comparable to the pyridine analog with low clearance ( $10.6 \text{ mL min}^{-1} \text{kg}^{-1}$ ) and good oral bioavailability (65%), Table 5. To further explore

**Table 5. Pharmacokinetics of Pyridine 14i and Pyrimidine 42**

compound	rat <sup>a</sup>		dog <sup>b</sup>		
	CL ( $\text{mL min}^{-1} \text{kg}^{-1}$ )	<i>F</i> (%)	PPB (%)	$C_{\text{max,free}}$ (nM)	AUC <sub>free</sub> (nM·h)
14i	7.7	48	76	66	1230
42	10.6	65	63	580	3240

<sup>a</sup>Rat: Crossover design, intravenous bolus administration (1.0 mg/kg,  $N = 2$ ), oral suspension administration (1.0 mg/kg,  $N = 2$ ). Complete rat pharmacokinetic parameters are available in Table S2 (Supporting Information). <sup>b</sup>Dog: Oral suspension administration to male beagle dogs in cassette dosing format (5 compounds, 1.0 mg/kg each,  $N = 3$ ).

potential differentiation, both compounds were dosed orally to dogs in a cassette experiment such that each animal received a dose equivalent to 1.0 mg/kg of **14i** and **42** in a single experiment. Pyrimidine **42** demonstrated a significantly better

oral absorption profile compared with the pyridine analog showing a more than 8-fold increase in free  $C_{\text{max}}$  exposure and a 2.6-fold increase in free AUC possibly driven by the improved aqueous solubility. Therefore, for the minimal increase in molecular weight by one mass unit, the transformation of pyridine to pyrimidine resulted in a significant improvement in lipophilic ligand efficiency ( $\Delta\text{LIPE} = 1.05$ ,  $\text{LIPE} = 6.94$ ) and pharmaceutical properties such as solubility and oral absorption while maintaining MMP-13 potency, selectivity, and metabolic stability.

Utilizing learnings from the benzamide substituent survey, the corresponding 4-fluoro-3-methoxybenzyl analog in the pyrimidine series was next targeted with the intent to further improve MMP-13 potency while maintaining the favorable pharmacokinetic properties. Both enantiomers (**2S,5R**)-**43a** and (**2R,5S**)-**43b** demonstrated excellent MMP-13 potency with **43a** being the more potent of the two (MMP-13  $K_i = 1.5$  nM), Table 6. High selectivity was maintained against MMP-3, and **43a** was further found to be highly selective against a panel of 14 matrix metalloproteinases, TACE, ADAMTS-4, and ADAMTS-5, Figure 3. Both enantiomers also showed favorable in vitro and rat in vivo pharmacokinetic profiles demonstrating low clearance and very high oral bioavailability, Table 6. The pharmacokinetics of enantiomer **43a** in dog and cynomolgus monkey was also favorable with low clearance (8.2 and 2.1  $\text{mL min}^{-1} \text{kg}^{-1}$ , respectively) and high oral bioavailability (64% and 88%, respectively). In in vitro metabolic drug–drug interaction assays, the  $\text{IC}_{50}$  of compound **43a** was  $>30 \mu\text{M}$  for the inhibition of CYPs 1A2, 2C9, 2D6, and 3A4.

Treatment of human articular cartilage ex-vivo cultures with cytokines results in the degradation of type II collagen and the production of a 45-amino acid fragment known as type II

**Table 6. Comparison of In Vitro and Pharmacokinetic Properties of 43a and 43b<sup>a</sup>**

compound	MMP-13/FL $K_i$ (nM)	MMP-3/CD $K_i$ (nM)	HLM <sup>b</sup> ( $\mu\text{L min}^{-1} \text{mg}^{-1}$ )	rat CL <sup>c</sup> ( $\text{mL min}^{-1} \text{kg}^{-1}$ )	rat <sup>c</sup> <i>F</i> (%)
43a	1.5	>10000	<8.0	18.2	95
43b	4.2	>10000	<8.0	9.8	113

<sup>a</sup>All in vitro values are the mean of two or more independent assays. <sup>b</sup>HLM in vitro intrinsic CL calculated from metabolic stability data as described in ref 21. <sup>c</sup>Rat: Crossover design, intravenous bolus administration (1.0 mg/kg,  $N = 2$ ), oral suspension administration (1.0 mg/kg,  $N = 2$ ). Complete rat pharmacokinetic parameters are available in Table S2 (Supporting Information).

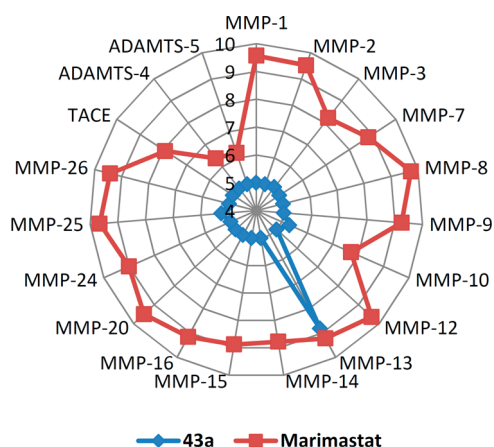


**Figure 3.** Metalloproteinase selectivity ( $pIC_{50}$ ) of **43a** compared with broad-spectrum agent marimastat (highest concentration tested  $10 \mu M$ ,  $pIC_{50} = 5$ ).

collagen neoepitope (TIINE). Compound **43a** (PF152) inhibited cytokine-induced TIINE production in a dose dependent manner.<sup>28</sup> The in vivo effect of compound **43a** on joint lesion progression was evaluated in the canine partial medial meniscectomy model of OA.<sup>28</sup> As a result of joint destabilization induced by the model, TIINE levels are increased and joint deterioration occurs. Administration of **43a** returned elevated TIINE levels to prestudy baseline suggesting suppression of MMP-13 mediated cartilage degradation in vivo. A corresponding reduction in the severity of the resulting OA-like joint lesions based on histological evaluation was also observed.

The hydroxymethyl substituent plays a necessary role in pharmacologic potency and in suppressing overall metabolism. However, in the latter it also poses a risk if oxidative metabolism results in the carboxylic acid metabolite, a species we were intending to avoid. In both rat and cynomolgus monkey PK studies, the carboxylic acid metabolite of **43a** (**45**) was present at very low levels, and the metabolite concentrations and half-life appeared to be dependent on the parent, Figure 4. As anticipated,

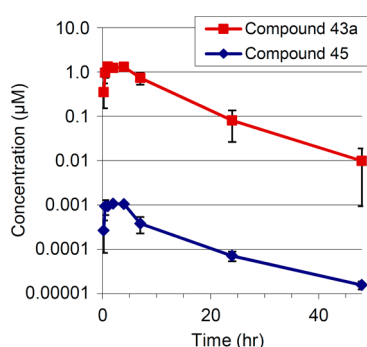


**Figure 4.** Mean plasma concentration–time profiles of **43a** and carboxylic acid metabolite **45** after oral administration of **43a** ( $1.0 \text{ mg/kg}$ ) to female cynomolgus monkeys ( $N = 3$ ).

carboxylic acid **45** has a lower in vitro  $K_i$  against human MMP-13 ( $0.2 \text{ nM}$ ) than **43a** ( $1.5 \text{ nM}$ ) and is thus presumed to be pharmacologically active. In cynomolgus monkey PK studies, the AUC ratio of parent/metabolite after oral dosing was 1460 at  $1 \text{ mg/kg}$  and 107 at  $100 \text{ mg/kg}$ . In in vitro incubations of **43a** in pooled human hepatocytes, at least six primary metabolites were identified. In addition to **45**, the metabolites resulted from

demethylation, methyl oxidation, and both a glucuronide and a sulfate conjugate were observed. These metabolites were also identified in cynomolgus monkey hepatocyte incubations and in in vivo cynomolgus monkey urine samples. Since hydroxymethyl oxidation was not the only observed metabolic pathway in human and cynomolgus monkey and exposures of **45** were predicted to be very low, we had sufficient confidence to proceed to an exploratory toxicology study to assess nephrotoxicity risk.

Compound **43a** was dosed orally ( $50$ ,  $100$ , and  $1000 \text{ mg kg}^{-1} \text{ day}^{-1}$ ) to cynomolgus monkeys for 14 days targeting free exposures that significantly exceeded efficacious levels observed in the canine OA model and the level where nephrotoxicity was observed with the previous carboxylic acid based MMP-13 inhibitor **6**. The compound was well tolerated and histological evaluation of the kidneys did not reveal abnormal pathology. Free exposures of **43a** achieved in the study were 22 times the projected efficacious AUC and 8.5 times an AUC exposure where nephrotoxicity was observed with compound **6**.

## CONCLUSION

We have shown that the carboxylic acid functional group found in previously disclosed highly selective MMP-13 inhibitors is not required to achieve excellent target potency, selectivity, and in vivo efficacy. The strategy to optimize nonacidic analogs of compound **6** has successfully identified inhibitor **43a** lacking the preclinical renal toxicity observed with previous lead molecules. Critical to achieving this milestone was the discovery that replacing the cyclohexane ring in initial leads with a dioxane ring could have a profound impact on metabolic susceptibility and overall pharmacokinetic properties. The use of a substituted dioxane ring to reduce lipophilicity and thus improve metabolic stability is an important tool medicinal chemists should consider when challenged by poor pharmacokinetics.

## EXPERIMENTAL SECTION

**General Methods.** All reagents and solvents were used as purchased without further purification. The purity of the final compounds was characterized by high-performance liquid chromatography (HPLC) using a gradient elution (C18 column, acetonitrile/water, 5/95–75/5, 5 min, 0.1% trifluoroacetic acid) and UV-detection ( $254 \text{ nm}$ ). The purity of all final compounds was 95% or greater. Proton ( $^1\text{H}$ ) NMR chemical shifts are referenced to a residual solvent peak.

***N-tert-Butyl-2-chloro-6-methylisonicotinamide*** (**9**). Oxalyl chloride ( $95 \text{ mL}$ ,  $1.10 \text{ mol}$ ) was added to a solution of **8** ( $95 \text{ g}$ ,  $0.55 \text{ mol}$ ) in dichloromethane ( $950 \text{ mL}$ , anhydrous). The mixture was cooled in an ice/water bath, and DMF ( $2.0 \text{ mL}$ ) was slowly added. When gas evolution subsided, the ice/water bath was removed, and the mixture was allowed to reach rt and stir for 15 h. The solution was then concentrated in vacuo and azeotropically distilled twice from toluene ( $200 \text{ mL}$ ) at reduced pressure. The residue was taken into dichloromethane ( $800 \text{ mL}$ , anhydrous) and cooled in an ice/water bath, and a solution of *tert*-butylamine ( $175 \text{ mL}$ ,  $1.7 \text{ mol}$ ) in dichloromethane ( $300 \text{ mL}$ , anhydrous) was added dropwise. The mixture was allowed to reach rt and stir for 15 h. The reaction mixture was diluted with water ( $250 \text{ mL}$ ). The organic layer was washed with water ( $200 \text{ mL}$ ) followed by brine ( $200 \text{ mL}$ ), dried ( $\text{MgSO}_4$ ), filtered, and concentrated to afford **120 g** (96%) of **9** as a beige solid.  $^1\text{H}$  NMR ( $400 \text{ MHz}$ ,  $\text{DMSO}-d_6$ )  $\delta$  7.39 (s, 1 H), 7.38 (s, 1 H), 6.05 (s, 1 H), 2.59 (s, 3 H), 1.5 (s, 9 H).

**2-Chloro-6-methylisonicotinonitrile** (**10**).  $\text{POCl}_3$  ( $572 \text{ mL}$ ,  $6.26 \text{ mol}$ ) was added to **9** ( $120 \text{ g}$ ,  $0.53 \text{ mol}$ ) in toluene ( $2.5 \text{ L}$ , anhydrous). The resulting mixture was refluxed 15 h, cooled to ambient temperature, and concentrated in vacuo. The residue was dissolved in dichloromethane ( $1.0 \text{ L}$ ) and aqueous saturated sodium bicarbonate ( $500 \text{ mL}$ ) was carefully added. Solid sodium bicarbonate was then added portionwise until the aqueous layer was basic. The organic layer was washed with brine ( $300 \text{ mL}$ ), dried ( $\text{MgSO}_4$ ), filtered, and concentrated

to afford 76 g (94%) of **10** as a pale tan solid.  $^1\text{H NMR}$  (400 MHz,  $\text{DMSO-}d_6$ )  $\delta$  7.41 (s, 1 H), 7.37 (s, 1 H), 2.61 (s, 3 H).

**2-Chloro-6-methyl-4-(2H-tetrazol-5-yl)pyridine hydrochloride (11).** Triethylamine hydrochloride (72 g, 0.52 mol) and sodium azide (34 g, 0.52 mol) were added to a solution of **10** (76 g, 0.50 mol) in toluene (1.2 L, anhydrous). The mixture was refluxed for 4 h behind a blast shield. **CAUTION!** Tetrazoles represent an explosion hazard at elevated temperatures. Adequate blast shielding is recommended. After cooling to rt, water (1.5 L) was added, and the layers were separated. The toluene layer was washed with water (500 mL), and the combined aqueous layers were acidified with 6 N HCl (100 mL). The resulting precipitate was filtered and dried in vacuo (60 °C) to afford 105 g (91%) of **11**.  $^1\text{H NMR}$  (400 MHz,  $\text{DMSO-}d_6$ )  $\delta$  7.92 (s, 1 H), 7.89 (s, 1 H), 2.79 (s, 3 H).

**Methyl 6-Methyl-4-(2H-tetrazol-5-yl)picolinate (12).** Triethylamine (120 mL, 1.63 mol), 1,1'-bis(diphenylphosphino)ferrocene (8.0 g, 14 mmol), and  $\text{Pd}(\text{OAc})_2$  (9.2 g, 40 mmol) were added to a solution of **11** (88 g, 380 mmol) in methanol (1.5 L, anhydrous) in a pressure reactor. The reactor was evacuated, purged with carbon monoxide gas twice, and finally pressurized to 120 PSI and heated to 100 °C for 24 h (190 PSI final pressure). **CAUTION!** Tetrazoles represent an explosion hazard at elevated temperatures. Adequate blast shielding is recommended. After cooling to rt, the mixture was filtered through Celite and concentrated in vacuo. Water (700 mL) and aqueous saturated sodium bicarbonate (200 mL) were added to dissolve all solids. HCl (3 N) was added until a pH of 2 was reached. The resulting solid was filtered and dried in vacuo (50 °C) to afford 78 g (94%) of **12** as a solid.  $^1\text{H NMR}$  (400 MHz,  $\text{DMSO-}d_6$ )  $\delta$  8.48 (s, 1 H), 8.15 (s, 1 H), 3.95 (s, 3 H), 2.67 (s, 3 H).

**N-(3-Methoxybenzyl)-6-methyl-4-(2H-tetrazol-5-yl)picolinamide (13).** A mixture of **12** (3.29 g, 15.0 mmol) and 3-methoxybenzylamine (6.17 g, 45.0 mmol) was heated at 100 °C with removal of methanol in a stream of nitrogen for 1 h. A solution of 1 N HCl (50 mL) was added. The resulting precipitate was filtered and washed with ethyl ether. The solid was suspended in a solution of 2.5 N sodium hydroxide (30 mL)/water (50 mL) and extracted with EtOAc (2 × 50 mL). The aqueous layer was cooled in an ice bath and acidified to pH 1 with concentrated HCl. The resulting precipitate was filtered and dried to afford 4.69 g (96%) of **13** as a white solid.  $^1\text{H NMR}$  (400 MHz,  $\text{DMSO-}d_6$ )  $\delta$  9.28 (t,  $J = 6.3$  Hz, 1 H), 8.49 (d,  $J = 0.8$  Hz, 1 H), 8.13 (d,  $J = 1.2$  Hz, 1 H), 7.24 (t,  $J = 8.1$  Hz, 1 H), 6.94–6.90 (m, 2 H), 6.82 (dd,  $J = 8.0, 2.1$  Hz, 1 H), 4.51 (d,  $J = 6.3$  Hz, 2 H), 3.73 (s, 3 H), 2.68 (s, 3 H). MS (ES+)  $m/z$  325 (M + H).

**4-(2-(Cyclohexylmethyl)-2H-tetrazol-5-yl)-N-(3-methoxybenzyl)-6-methylpicolinamide (14b).** Polymer supported triphenylphosphine (698 mg, 1.5 mmol, 1.5 equiv), **13** (324 mg, 1.0 mmol), and cyclohexylmethanol (137 mg, 1.2 mmol, 1.2 equiv) were suspended in THF (16 mL). DBAD (345 mg, 1.5 mmol, 1.5 equiv) was added. The mixture was allowed to stir for 18 h. The reaction mixture was filtered, and the resin was washed with THF (20 mL). The filtrate was concentrated. The crude product was purified by column chromatography (heptane/EtOAc, 6/1; 4/1) to afford 248 mg (49%) of **14b** as an oil.  $^1\text{H NMR}$  (400 MHz,  $\text{DMSO-}d_6$ )  $\delta$  9.29 (t,  $J = 6.4$  Hz, 1 H), 8.43 (s, 1 H), 8.09 (s, 1 H), 7.25 (t,  $J = 8.0$  Hz, 1 H), 6.96–6.89 (m, 2 H), 6.82 (dd,  $J = 8.2, 2.4$  Hz, 1 H), 4.67 (d,  $J = 7.0$  Hz, 2 H), 4.51 (d,  $J = 6.3$  Hz, 2 H), 3.74 (s, 3 H), 2.68 (s, 3 H), 2.08–1.99 (m, 1 H), 1.74–1.54 (m, 5 H), 1.29–1.00 (m, 4 H). MS (ES+)  $m/z$  421 (M + H).

**(-)-N-(3-Methoxybenzyl)-6-methyl-4-(2-((tetrahydro-2H-pyran-2-yl)methyl)-2H-tetrazol-5-yl)picolinamide (14c).** Following conditions analogous to those described for **14b**, reaction of tetrahydropyran-2-methanol (0.348 mL, 3.08 mmol) afforded the racemic product, which was resolved by SFC (Chiralcel OD-H, 30 mm × 250 mm, 25/75 ethanol/ $\text{CO}_2$ , 70 mL/min). Isolation of the first eluting isomer afforded 250 mg (39%) of **14c** as an oil. Chiralcel OD-H analytical column (4.6 mm × 250 mm; 20/80, ethanol/ $\text{CO}_2$ ), 8.06 min, > 99% ee;  $[\alpha]_D^{25} = -22.7^\circ$  ( $c = 8.3$ , DMF).  $^1\text{H NMR}$  (400 MHz,  $\text{DMSO-}d_6$ )  $\delta$  9.23 (m, 1 H), 8.40 (s, 1 H), 8.05 (s, 1 H), 7.23–7.19 (m, 1 H), 6.89–6.87 (m, 2 H), 6.80–6.77 (m, 1 H), 4.79–4.74 (m, 2 H), 4.48 (d,  $J = 6.0$  Hz, 2 H), 3.93–3.75 (m, 3 H), 3.70 (s, 3 H), 2.65 (s, 3 H), 1.80–1.25 (m, 6 H). MS (ES+)  $m/z$  423 (M + H).

**(+)-N-(3-Methoxybenzyl)-6-methyl-4-(2-((tetrahydro-2H-pyran-2-yl)methyl)-2H-tetrazol-5-yl)picolinamide (14d).** Isolation of the second eluting isomer from above afforded 260 mg (41%) of **14d** as an oil. Chiralcel OD-H analytical column (4.6 mm × 250 mm; 20/80, ethanol/ $\text{CO}_2$ ), 9.99 min, > 99% ee;  $[\alpha]_D^{25} = 19.0^\circ$  ( $c = 9.8$ , DMF).  $^1\text{H NMR}$  (400 MHz,  $\text{DMSO-}d_6$ )  $\delta$  9.23 (m, 1 H), 8.40 (s, 1 H), 8.05 (s, 1 H), 7.23–7.19 (m, 1 H), 6.89–6.87 (m, 2 H), 6.80–6.77 (m, 1 H), 4.79–4.74 (m, 2 H), 4.48 (d,  $J = 6.0$  Hz, 2 H), 3.93–3.75 (m, 3 H), 3.70 (s, 3 H), 2.65 (s, 3 H), 1.80–1.25 (m, 6 H). MS (ES+)  $m/z$  423 (M + H).

**rac-N-(3-Methoxybenzyl)-6-methyl-4-(2-((tetrahydro-2H-pyran-3-yl)methyl)-2H-tetrazol-5-yl)picolinamide (14e).** A mixture of **13** (79 mg, 0.23 mmol), **15** (77 mg, 0.25 mmol), and triethylamine (0.40 mL) in DMA (0.1 mL) was stirred at 85 °C for 15 h. The reaction mixture was purified by reverse phase preparative HPLC to afford 62 mg (61%) of **14e** as a solid.  $^1\text{H NMR}$  (400 MHz,  $\text{DMSO-}d_6$ )  $\delta$  9.20 (br. s., 1 H), 8.08 (s, 1 H), 7.24 (t,  $J = 8.1$  Hz, 1 H), 6.93 (br. s., 2 H), 6.82 (d,  $J = 7.7$  Hz, 1 H), 4.75 (dq,  $J = 13.0, 6.8$  Hz, 2 H), 4.51 (d,  $J = 6.2$  Hz, 2 H), 3.73 (s, 5 H), 3.68 (br. s., 1 H), 3.41 (br. s., 1 H), 3.37 (d,  $J = 2.2$  Hz, 1 H), 2.68 (s, 3 H), 2.28 (br. s., 1 H), 1.74 (br. s., 1 H), 1.62 (br. s., 1 H), 1.50 (d,  $J = 8.8$  Hz, 1 H), 1.35 (d,  $J = 9.5$  Hz, 1 H). MS (ES+)  $m/z$  423 (M + H).

**rac-4-(2-((1,4-Dioxan-2-yl)methyl)-2H-tetrazol-5-yl)-N-(3-methoxybenzyl)-6-methylpicolinamide (14f).** Following conditions analogous to those described for **14b**, reaction of *rac*-(1,4-dioxan-2-yl)methanol (142 mg, 1.2 mmol) afforded 250 mg (59%) of **14f** as an oil.  $^1\text{H NMR}$  (400 MHz,  $\text{DMSO-}d_6$ )  $\delta$  9.29 (t,  $J = 6.5$  Hz, 1 H), 8.44 (s, 1 H), 8.10 (s, 1 H), 7.25 (t,  $J = 8.1$  Hz, 1 H), 6.95–6.90 (m, 2 H), 6.82 (dd,  $J = 8.2, 2.6$  Hz, 1 H), 4.96–4.85 (m, 2 H), 4.51 (d,  $J = 6.3$  Hz, 2 H), 4.19–4.11 (m, 1 H), 3.92 (dd,  $J = 11.4, 2.4$  Hz, 1 H), 3.74 (s, 5 H), 3.58–3.40 (m, 3 H), 2.69 (s, 3 H). MS (ES+)  $m/z$  425 (M + H).

**N-(3-Methoxybenzyl)-4-(2-(((trans)-4-(hydroxymethyl)cyclohexyl)methyl)-2H-tetrazol-5-yl)-6-methylpicolinamide (14g).** Following conditions analogous to those described for **14b**, reaction of *trans*-cyclohexane-1,4-dimethanol (178 mg, 1.23 mmol) afforded 102 mg (37%) of **14g** as a white solid.  $^1\text{H NMR}$  (400 MHz,  $\text{DMSO-}d_6$ )  $\delta$  9.23 (m, 1 H), 8.39 (s, 1 H), 8.05 (s, 1 H), 7.12–7.28 (m, 1 H), 6.94–6.84 (m, 2 H), 6.82–6.72 (m, 1 H), 4.63 (d,  $J = 7.0$  Hz, 2 H), 4.47 (d,  $J = 6.4$  Hz, 2 H), 3.70 (s, 3 H), 3.21–3.08 (m, 2 H), 2.64 (s, 3 H), 2.04–1.81 (m, 1 H), 1.78–1.50 (m, 4 H), 1.43–1.16 (m, 2 H), 1.15–0.71 (m, 4 H). MS (ES+)  $m/z$  451 (M + H).

**N-(3-Methoxybenzyl)-4-(2-(((cis)-4-(hydroxymethyl)cyclohexyl)methyl)-2H-tetrazol-5-yl)-6-methylpicolinamide (14h).** Following conditions analogous to those described for **14b**, reaction of *cis*-cyclohexane-1,4-dimethanol (89 mg, 0.62 mmol) afforded 62 mg (45%) of **14h** as an oil.  $^1\text{H NMR}$  (400 MHz,  $\text{DMSO-}d_6$ )  $\delta$  9.26 (t,  $J = 6.4$  Hz, 1 H), 8.42 (d,  $J = 0.9$  Hz, 1 H), 8.08 (d,  $J = 1.1$  Hz, 1 H), 7.24 (t,  $J = 8.1$  Hz, 1 H), 6.93–6.90 (m, 2 H), 6.82 (ddd,  $J = 8.2, 2.5, 0.9$  Hz, 1 H), 4.76 (d,  $J = 7.7$  Hz, 2 H), 4.51 (d,  $J = 6.4$  Hz, 2 H), 4.37 (t,  $J = 5.4$  Hz, 1 H), 3.73 (s, 3 H), 3.33 (dd,  $J = 6.4, 5.5$  Hz, 2 H), 2.68 (s, 3 H), 2.31–2.21 (m, 1 H), 1.65–1.27 (m, 9 H). MS (ES+)  $m/z$  351 (M + H).

**rac-N-(3-Methoxybenzyl)-4-(2-(((2S\*,5R\*)-5-(hydroxymethyl)-1,4-dioxan-2-yl)methyl)-2H-tetrazol-5-yl)-6-methylpicolinamide (14i).** Tosylate **16** (1.4 g, 4.3 mmol) was added to a mixture of **13** (1.0 g, 3.1 mmol) and triethylamine (0.4 g, 4.0 mmol) in anhydrous DMA (1 mL). The mixture was stirred at 85 °C overnight and then was purified by reverse phase preparative HPLC to afford 1.04 g (70%) of **14i** as a white solid.  $^1\text{H NMR}$  (400 MHz,  $\text{DMSO-}d_6$ )  $\delta$  9.20 (t,  $J = 6.2$  Hz, 1 H), 8.43 (s, 1 H), 8.08 (s, 1 H), 7.24 (t,  $J = 8.1$  Hz, 1 H), 6.93 (br. s., 2 H), 6.83 (d,  $J = 1.5$  Hz, 1 H), 4.80–4.95 (m, 2 H), 4.65 (t,  $J = 5.7$  Hz, 1 H), 4.52 (d,  $J = 6.2$  Hz, 2 H), 4.05–4.15 (m, 1 H), 3.99 (dd,  $J = 11.3, 1.8$  Hz, 1 H), 3.77 (d,  $J = 11.3$  Hz, 1 H), 3.73 (s, 3 H), 3.30–3.50 (m, 4 H), 2.68 (s, 3 H). MS (ES+)  $m/z$  455 (M + H).

**N-(3-Methoxybenzyl)-4-(2-(((trans)-4-(hydroxycyclohexyl)methyl)-2H-tetrazol-5-yl)-6-methylpicolinamide (14j).** Following conditions analogous to those described for **14b**, reaction of 4-(hydroxymethyl)cyclohexanol (614 mg, 4.7 mmol) afforded a mixture of isomers, which was purified by reverse phase preparative HPLC (acetonitrile/water, 35/65–55/45). Isolation of the first eluting isomer afforded 298 mg (22%) of **14j**.  $^1\text{H NMR}$  (400 MHz,  $\text{DMSO-}d_6$ )  $\delta$  9.19

(*t*, *J* = 6.4 Hz, 1 H), 8.40 (s, 1 H), 8.05 (s, 1 H), 7.22 (*t*, *J* = 8.1 Hz, 1 H), 6.87–6.92 (m, 2 H), 6.77–6.82 (m, 1 H), 4.63 (d, *J* = 7.0 Hz, 2 H), 4.49 (d, *J* = 6.2 Hz, 2 H), 3.71 (s, 3 H), 2.65 (s, 3 H), 2.52 (s, 1 H), 1.89–1.98 (m, 1 H), 1.77–1.85 (m, 2 H), 1.53–1.61 (m, 2 H), 1.37 (d, *J* = 7.3 Hz, 2 H), 1.03–1.17 (m, 2 H). MS (ES+) *m/z* 437 (M + H).

***N*-(3-Methoxybenzyl)-4-(2-(((*cis*)-4-hydroxycyclohexyl)-methyl)-2*H*-tetrazol-5-yl)-6-methylpicolinamide (14k).** Isolation of the second eluting isomer from the reaction above afforded 520 mg (39%) of **14k**. <sup>1</sup>H NMR (400 MHz, DMSO-*d*<sub>6</sub>) δ 9.19 (*t*, *J* = 6.4 Hz, 1 H), 8.40 (s, 1 H), 8.05 (s, 1 H), 7.21 (*t*, *J* = 8.1 Hz, 1 H), 6.87–6.92 (m, 2 H), 6.79 (dd, *J* = 8.4, 1.5 Hz, 1 H), 4.65 (d, *J* = 7.0 Hz, 2 H), 4.48 (d, *J* = 6.6 Hz, 2 H), 4.30 (br. s., 1 H), 3.73 (br. s., 1 H), 3.71 (s, 3 H), 2.65 (s, 3 H), 2.52 (s, 1 H), 2.04 (br. s., 1 H), 1.54–1.63 (m, 2 H), 1.27–1.48 (m, 5 H). MS (ES+) *m/z* 437 (M + H).

***rac*-(Tetrahydro-2*H*-pyran-3-yl)methyl 4-Nitrobenzenesulfonate (15).** 4-Nitrobenzene-1-sulfonyl chloride (0.62 g, 2.8 mmol) and pyridine (253 mg, 3.20 mmol) were added to a solution of *rac*-(tetrahydro-2*H*-pyran-3-yl)methanol (0.31 g, 2.67 mmol) in dichloromethane (5 mL), and the mixture was stirred at rt for 15 h. The reaction mixture was diluted with dichloromethane (10 mL) and washed with water (2 × 10 mL) and brine (10 mL), dried over sodium sulfate, filtered, and concentrated. The residue was purified on silica gel column chromatography (heptane/EtOAc, 100/0–50/50) to afford 0.65 g (81%) of **15** as an oil. MS (ES+) *m/z* 302 (M + H).

***rac*-(2*R*\*,5*R*\*)-5-(Hydroxymethyl)-1,4-dioxan-2-yl)methyl 4-Methylbenzenesulfonate (*rac*-16).** *trans*-2,5-Bis(hydroxymethyl)-1,4-dioxane (342.9 g, 2.31 mol), <sup>20</sup> *p*-toluene sulfonyl chloride (441.0 g, 2.31 mol), triethylamine (471.5 g, 4.66 mol), and dichloromethane (3 L) were combined in a 5 L round-bottomed flask equipped with a mechanical stirrer under nitrogen. The mixture was maintained at 35 °C for 30 min with water bath cooling (**CAUTION! Exothermic reaction**) and then allowed to stir at rt overnight. The mixture was diluted with 3 N HCl (1 L), and the resulting solids were filtered. The organic phase of the filtrate was separated, washed with 3 N HCl (1 L) followed by saturated ammonium chloride solution (500 mL), dried (MgSO<sub>4</sub>), and concentrated to afford 338.3 g (48%) of *rac*-**16** as a white solid. <sup>1</sup>H NMR (400 MHz, CDCl<sub>3</sub>) δ 7.77 (d, *J* = 8.1 Hz, 2 H), 7.33 (d, *J* = 8.1 Hz, 2 H), 3.90–4.02 (m, 2 H), 3.37–3.86 (m, 9 H), 2.43 (s, 3 H). MS (ES+) *m/z* 303 (M + H).

**Chiral Resolution of *rac*-16.** Chromatographic separation of *rac*-**16** by chiral SFC (AD-H; 30% methanol/dichloromethane, 10/1; 200 mL/min) was performed. Isolation of the first eluting isomer afforded (**2*R*,5*R***)-**16** (>99% ee) as a white solid. Isolation of the second eluting isomer afforded (**2*S*,5*S***)-**16** (>99% ee) as a white solid.

**(*trans*)-Methyl 4-(((5-(2-(((3-Methoxybenzyl)carbamoyl)-6-methylpyridin-4-yl)-2*H*-tetrazol-2-yl)methyl)-cyclohexanecarboxylate (17).** Following conditions analogous to those described for **14b**, reaction of methyl *trans*-4-(hydroxymethyl)-cyclohexanecarboxylate (2.12 g, 12.33 mmol) afforded 1.58 g (54%) of **17** as a white solid. <sup>1</sup>H NMR (400 MHz, DMSO-*d*<sub>6</sub>) δ 9.26 (*t*, *J* = 6.44 Hz, 1 H), 8.42 (s, 1 H), 8.07 (s, 1 H), 7.24 (*t*, *J* = 8.19 Hz, 1 H), 6.97–6.88 (m, 2 H), 6.86–6.77 (m, 1 H), 4.67 (d, *J* = 6.98 Hz, 2 H), 4.51 (d, *J* = 6.18 Hz, 2 H), 3.73 (s, 3 H), 3.57 (s, 3 H), 2.67 (s, 3 H), 2.31–2.19 (m, 1 H), 2.08–1.95 (m, 1 H), 1.95–1.84 (m, 2 H), 1.70–1.58 (m, 2 H), 1.39–1.25 (m, 2 H), 1.21–1.06 (m, 2 H). MS (ES+) *m/z* 479 (M + H).

***N*-(3-Methoxybenzyl)-4-(2-(((*trans*)-4-carbamoylcyclohexyl)-methyl)-2*H*-tetrazol-5-yl)-6-methylpicolinamide (18).** Formamide (120 mg) was added to a solution of **17** (100 mg, 0.2 mmol) in anhydrous tetrahydrofuran (1 mL) and the mixture was heated to reflux. A 25% sodium methoxide solution in methanol (120 mg) was added, and the reaction was stirred at reflux for 2 h. The reaction mixture was allowed to cool to rt and then diluted with methanol (2 mL). The resulting precipitate was filtered and washed with a small amount of methanol, and the solid was dried in a vacuum desiccator to afford 78 mg (85%) of **18** as a white solid. <sup>1</sup>H NMR (400 MHz, DMSO-*d*<sub>6</sub>) δ 9.22 (*t*, *J* = 6.6 Hz, 1 H), 8.4 (s, 1 H), 8.05 (s, 1 H), 7.21 (*t*, *J* = 8.2 Hz, 1 H), 7.15 (s, 1 H), 6.88 (m, 2 H), 6.79 (d, *J* = 8.1 Hz, 1 H), 6.61 (s, 1 H), 4.62 (d, *J* = 7.4, 2 H), 4.46 (d, *J* = 7.4, 2 H), 3.70 (s, 3 H), 2.62 (s, 3 H), 2.02–1.90 (m, 2 H), 1.68 (d, *J* = 13.6, 2 H), 1.60 (d, *J* = 13.1, 2 H), 1.35–1.20 (m, 2 H), 1.15–1.00 (m, 2 H). MS (ES+) *m/z* 464 (M + H).

***N*-(3-Methoxybenzyl)-4-(2-(((*trans*)-4-cyanocyclohexyl)-methyl)-2*H*-tetrazol-5-yl)-6-methylpicolinamide (19).** Polymer supported triphenylphosphine (500 mg, 1.07 mmol) was added to **18** (77 mg, 0.16 mmol) in a mixture of carbon tetrachloride (0.5 mL) and DCE (4.5 mL), and the mixture was heated at 80 °C for 2 h. The reaction mixture was filtered, and the resin was washed with DCE. The filtrate was concentrated, and the residue was recrystallized from methanol to afford **19** as a white solid. <sup>1</sup>H NMR (400 MHz, DMSO-*d*<sub>6</sub>) δ 9.29 (*t*, *J* = 6.6 Hz, 1 H), 8.43 (s, 1 H), 8.09 (s, 1 H), 7.25 (*t*, *J* = 8.0 Hz, 1 H), 6.90–6.94 (m, 2 H), 6.83 (dd, *J* = 8.1, 2.3 Hz, 1 H), 4.69 (d, *J* = 6.8 Hz, 2 H), 4.51 (d, *J* = 6.5 Hz, 2 H), 3.74 (s, 3 H), 2.68 (s, 3 H), 2.59–2.67 (m, 1 H), 1.98–2.13 (m, 3 H), 1.65 (d, *J* = 13.1 Hz, 2 H), 1.45–1.56 (m, 2 H), 1.07–1.19 (m, 2 H). MS (ES+) *m/z* 446 (M + H).

***tert*-Butyl (*trans*)-4-(((5-(2-(((3-Methoxybenzyl)carbamoyl)-6-methylpyridin-4-yl)-2*H*-tetrazol-2-yl)methyl)-cyclohexylcarbamate (21).** Following conditions analogous to those described for **14b**, reaction of *tert*-butyl *trans*-(4-hydroxymethyl)-cyclohexylcarbamate **20** (1.38 g, 6.0 mmol) provided a crude product, which was purified by silica column chromatography (CH<sub>2</sub>Cl<sub>2</sub>/methanol, 100/1; 100/2) to afford 1.824 g (68%) of **21** as a white solid. <sup>1</sup>H NMR (400 MHz, DMSO-*d*<sub>6</sub>) δ 9.23 (*t*, *J* = 6.3 Hz, 1 H), 8.40 (d, *J* = 0.8 Hz, 1 H), 8.05 (d, *J* = 1.1 Hz, 1 H), 7.21 (*t*, *J* = 8.1 Hz, 1 H), 6.90–6.86 (m, 2 H), 6.79 (dd, *J* = 8.2, 1.9 Hz, 1 H), 6.68 (d, *J* = 7.8 Hz, 1 H), 4.63 (d, *J* = 7.0 Hz, 2 H), 4.48 (d, *J* = 6.3 Hz, 2 H), 3.70 (s, 3 H), 3.13 (br. s., 1 H), 2.64 (s, 3 H), 1.90 (br. s., 1 H), 1.77–1.71 (m, 2 H), 1.59–1.53 (m, 2 H), 1.33 (s, 9 H), 1.14–1.06 (m, 4 H). MS (ES+) *m/z* 536 (M + H).

***N*-(3-Methoxybenzyl)-4-(2-(((*trans*)-4-aminocyclohexyl)-methyl)-2*H*-tetrazol-5-yl)-6-methylpicolinamide (22).** Trifluoroacetic acid (5.05 mL, 68.0 mmol) was added to a solution of **21** (1.82 g, 3.40 mmol) in dichloromethane (20 mL). The mixture was allowed to stir for 2 h and was then concentrated. The residue was dissolved in dichloromethane (150 mL) and washed with 1 N NaOH solution (2 × 40 mL). The organic layer was dried (Na<sub>2</sub>SO<sub>4</sub>) and concentrated. The residue was triturated with heptane and filtered to afford 1.41 g (95%) of **22** as a white solid. <sup>1</sup>H NMR (400 MHz, DMSO-*d*<sub>6</sub>) δ 9.23 (*t*, *J* = 6.3 Hz, 1 H), 8.39 (d, *J* = 0.8 Hz, 1 H), 8.05 (d, *J* = 1.2 Hz, 1 H), 7.21 (*t*, *J* = 8.1 Hz, 1 H), 6.90–6.86 (m, 2 H), 6.79 (dd, *J* = 8.2, 1.9 Hz, 1 H), 4.62 (d, *J* = 7.1 Hz, 2 H), 4.48 (d, *J* = 6.3 Hz, 2 H), 3.70 (s, 3 H), 2.64 (s, 3 H), 2.45–2.37 (m, 1 H), 1.96–1.84 (m, 1 H), 1.71 (d, *J* = 12.0 Hz, 2 H), 1.53 (d, *J* = 12.2 Hz, 2 H), 1.37 (br. s., 2 H), 1.07 (q, *J* = 12.8 Hz, 2 H), 1.01–0.88 (m, 2 H). MS (ES+) *m/z* 436 (M + H).

***N*-(3-Methoxybenzyl)-6-methyl-4-(2-(((*trans*)-4-(methylsulfonamido)cyclohexyl)methyl)-2*H*-tetrazol-5-yl)-picolinamide (23a).** Triethylamine (0.096 mL, 0.690 mmol) and methane sulfonyl chloride (0.021 mL, 0.276 mmol) were added to a solution of **22** (100.0 mg, 0.230 mmol) in dichloromethane (2 mL). The mixture was stirred for 2 h at rt and then concentrated. The residue was purified by reverse phase preparative HPLC to afford 28 mg (24%) of **23a** as a solid. <sup>1</sup>H NMR (400 MHz, DMSO-*d*<sub>6</sub>) δ 9.31–9.04 (m, 1 H), 8.41 (s, 1 H), 8.05 (s, 1 H), 7.29–7.12 (m, 1 H), 6.93 (s, 1 H), 6.90 (m, 2 H), 6.82–6.77 (m, 1 H), 4.64 (d, *J* = 7.3 Hz, 2 H), 4.49 (d, *J* = 5.9 Hz, 2 H), 3.71 (s, 3 H), 2.86 (s, 3 H), 2.65 (s, 3 H), 2.04–1.78 (m, 3 H), 1.69–1.49 (m, 2 H), 1.32–0.95 (m, 4 H). MS (ES+) *m/z* 514 (M + H).

***N*-(3-Methoxybenzyl)-4-(2-(((*trans*)-4-acetamidocyclohexyl)-methyl)-2*H*-tetrazol-5-yl)-6-methylpicolinamide (23b).** Acetic anhydride (0.033 mL, 0.344 mmol) and silica-bound DMAP (833.0 mg, 0.575 mmol, 0.69 mmol/g loading) were added to a solution of **22** (50.1 mg, 0.115 mmol) in dichloromethane (2 mL). The reaction mixture was stirred overnight at rt, filtered, and washed with DMF. The filtrate was concentrated, and the residue was purified by reverse phase preparative HPLC to afford 22.4 mg (41%) of **23b**. <sup>1</sup>H NMR (400 MHz, DMSO-*d*<sub>6</sub>) δ 9.26–9.09 (m, 1 H), 8.41 (s, 1 H), 8.05 (s, 1 H), 7.63 (s, 1 H), 7.30–7.13 (m, 1 H), 6.98–6.86 (m, 2 H), 6.83–6.75 (m, 1 H), 4.64 (d, *J* = 7.3 Hz, 2 H), 4.49 (d, *J* = 5.9 Hz, 2 H), 3.71 (s, 3 H), 2.65 (s, 3 H), 2.06–1.89 (m, 1 H), 1.81–1.74 (m, 3 H), 1.73 (s, 3 H), 1.60 (m, 2 H), 1.28–0.99 (m, 4 H). MS (ES+) *m/z* 478 (M + H).

***tert*-Butyl (*cis*)-4-(((5-(2-(((3-Methoxybenzyl)carbamoyl)-6-methylpyridin-4-yl)-2*H*-tetrazol-2-yl)methyl)-cyclohexylcarbamate (25).** Following conditions analogous to those

described for **14b**, reaction of *tert*-butyl *cis*-(4-hydroxymethyl)cyclohexylcarbamate **24** (1.41 g, 6.17 mmol) provided a crude product, which was purified by reverse phase preparative HPLC to afford 1.65 g (50%) of **25** as a solid. MS (ES+) *m/z* 480 (M - C<sub>4</sub>H<sub>8</sub>).

**N-(3-Methoxybenzyl)-4-(2-(((*cis*)-4-aminocyclohexyl)methyl)-2H-tetrazol-5-yl)-6-methylpicolinamide (26)**. Trifluoroacetic acid was added to a solution of **25** (1.65 g, 3.1 mmol) in dichloromethane, and the mixture was allowed to stir for 30 min at rt. The reaction mixture was concentrated. The residue was dissolved in dichloromethane, and MP-carbonate resin was added. The mixture was agitated for 1 h, filtered, and washed with dichloromethane and methanol. The filtrate was concentrated to afford 1.09 g (81%) of **26** as a solid. <sup>1</sup>H NMR (400 MHz, DMSO-*d*<sub>6</sub>) δ 9.28–9.19 (m, 1 H), 8.41 (s, 1 H), 8.09–8.03 (m, 1 H), 7.93 (br. s., 2 H), 7.27–7.17 (m, 1 H), 6.93–6.85 (m, 2 H), 6.84–6.76 (m, 1 H), 4.72 (d, *J* = 7.3 Hz, 2 H), 4.48 (d, *J* = 6.4 Hz, 2 H), 3.70 (s, 3 H), 3.28–3.18 (m, 1 H), 2.65 (s, 3 H), 2.31–2.17 (m, 1 H), 1.86–1.33 (m, 8 H). MS (ES+) *m/z* 436 (M + H).

**N-(3-Methoxybenzyl)-6-methyl-4-(2-(((*cis*)-4-(methylsulfonamidocyclohexyl)methyl)-2H-tetrazol-5-yl)picolinamide (27a)**. Compound **27a** was prepared analogous to **23a** from compound **26**. Yield 57%. <sup>1</sup>H NMR (400 MHz, DMSO-*d*<sub>6</sub>) δ 9.25–9.12 (m, 1 H), 8.41 (s, 1 H), 8.05 (s, 1 H), 7.28–7.13 (m, 1 H), 6.97–6.84 (m, 3 H), 6.84–6.73 (m, 1 H), 4.67 (d, *J* = 6.6 Hz, 2 H), 4.49 (d, *J* = 6.6 Hz, 2 H), 3.71 (s, 3 H), 3.48–3.36 (m, 1 H), 2.87 (s, 3 H), 2.65 (s, 3 H), 2.22–1.99 (m, 1 H), 1.79–1.29 (m, 4 H). MS (ES+) *m/z* 514 (M + H).

**N-(3-Methoxybenzyl)-4-(2-(((*cis*)-4-acetamidocyclohexyl)methyl)-2H-tetrazol-5-yl)-6-methylpicolinamide (27b)**. Compound **27b** was prepared analogous to **23b** from compound **26**. Yield 49%. <sup>1</sup>H NMR (400 MHz, DMSO-*d*<sub>6</sub>) δ 9.23–9.14 (m, 1 H), 8.41 (s, 1 H), 8.05 (s, 1 H), 7.68–7.60 (m, 1 H), 7.25–7.17 (m, 1 H), 6.94–6.86 (m, 2 H), 6.82–6.76 (m, 1 H), 4.68 (d, *J* = 7.3 Hz, 2 H), 4.49 (d, *J* = 6.6 Hz, 2 H), 3.82–3.74 (m, 1 H), 3.71 (s, 3 H), 3.31–3.23 (m, 1 H), 2.69–2.62 (m, 3 H), 2.21–2.07 (m, 1 H), 1.80 (s, 3 H), 1.66–1.31 (m, 3 H). MS (ES+) *m/z* 478 (M + H).

**tert-Butyl 4-((5-(2-((3-methoxybenzyl)carbamoyl)-6-methylpyridin-4-yl)-2H-tetrazol-2-yl)methyl)piperidine-1-carboxylate (29)**. A mixture of **28** (1.00 g, 3.10 mmol), *tert*-butyl 4-(hydroxymethyl)piperidine-1-carboxylate (0.81 g, 3.8 mmol), and polymer supported-triphenylphosphine (2.90 g, 6.21 mmol) were suspended in anhydrous THF (32 mL). The mixture was cooled to 0 °C in an ice bath for 15 min, and then DBAD (1.11 g, 4.82 mmol) was added. The mixture was allowed to warm to rt while stirring over 15 h. The reaction mixture was filtered, and the filtrate was concentrated. The residue was purified by silica gel chromatography (20 g, 0–50% gradient EtOAc/heptane) to afford 1.52 g (94%) of **29** as a white solid. <sup>1</sup>H NMR (400 MHz, DMSO-*d*<sub>6</sub>) δ 9.22 (t, *J* = 8.0 Hz, 1 H), 8.40 (s, 1 H), 8.08 (s, 1 H), 7.22 (t, *J* = 8.2 Hz, 1 H), 6.90 (m, 2 H), 6.80 (m, 1 H), 4.78 (d, *J* = 7.0 Hz, 2 H), 4.50 (d, *J* = 7.0 Hz, 2 H), 4.00–3.90 (m, 2 H), 3.75 (s, 3 H), 2.68 (s, 3 H), 2.25–2.15 (m, 1 H), 1.60–1.50 (m, 2 H), 1.38 (s, 9 H), 1.20–1.10 (m, 2 H). MS (ES+) *m/z* 544 (M + Na).

**N-(3-Methoxybenzyl)-6-methyl-4-(2-(piperidin-4-ylmethyl)-2H-tetrazol-5-yl)picolinamide (30)**. Trifluoroacetic acid (6 mL) was added to a solution of **29** (1.51 g, 2.89 mmol) in dichloromethane (20 mL). The reaction mixture was stirred for 1 h at rt and was then concentrated. The residue was purified by reverse phase preparative HPLC to afford 0.83 g (56%) of **30** as the trifluoroacetate salt. MS (ES+) *m/z* 422 (M + H).

**N-(3-Methoxybenzyl)-4-(2-((1-acetylpiperidin-4-yl)methyl)-2H-tetrazol-5-yl)-6-methylpicolinamide (31a)**. Acetic anhydride (0.034 mL, 0.356 mmol) and silica-bound DMAP (862.0 mg, 0.595 mmol, 0.69 mmol/g loading) were added to a solution of **30** (50.2 mg, 0.119 mmol) in dichloromethane (2 mL), and the mixture was agitated overnight at rt. The reaction mixture was filtered, and the resin was washed with DMF. The filtrate was concentrated, and the residue was purified by reverse phase preparative HPLC to afford 24.5 mg (44%) of **31a** as a solid. <sup>1</sup>H NMR (400 MHz, DMSO-*d*<sub>6</sub>) δ 9.27–9.11 (m, 1 H), 8.41 (s, 1 H), 8.05 (s, 1 H), 7.28–7.14 (m, 1 H), 6.95–6.86 (m, 2 H), 6.80 (m, 1 H), 4.71 (d, *J* = 7.3 Hz, 2 H), 4.49 (d, *J* = 6.6 Hz, 2 H), 3.71 (s, 3 H), 2.65 (s, 3 H), 2.57–2.44 (m, 2 H), 2.37–2.16 (m, 1 H), 1.94 (s, 3 H), 1.57 (m, 2 H), 1.35–0.98 (m, 4 H). MS (ES+) *m/z* 464 (M + H).

**N-(3-Methoxybenzyl)-6-methyl-4-(2-((1-(methylsulfonyl)piperidin-4-yl)methyl)-2H-tetrazol-5-yl)picolinamide (31b)**. Compound **31b** was prepared analogous to **31a** employing methane sulfonyl chloride. Yield 55%. <sup>1</sup>H NMR (400 MHz, DMSO-*d*<sub>6</sub>) δ 9.19 (s, 1 H), 8.41 (s, 1 H), 8.05 (s, 1 H), 7.27–7.15 (m, 1 H), 6.95–6.86 (m, 2 H), 6.83–6.73 (m, 1 H), 4.76 (d, *J* = 7.3 Hz, 2 H), 4.49 (d, *J* = 6.6 Hz, 2 H), 3.71 (s, 3 H), 3.60–3.47 (m, 2 H), 2.81 (s, 3 H), 2.65 (s, 3 H), 2.27–2.07 (m, 1 H), 1.72–1.61 (m, 2 H), 1.48–1.24 (m, 4 H). MS (ES+) *m/z* 500 (M + H).

**Methyl 4-(2-(((*trans*)-4-(hydroxymethyl)cyclohexyl)methyl)-2H-tetrazol-5-yl)-6-methylpicolinate (32)**. DBAD (4.6 g, 20.0 mmol) was added to a mixture of **13** (2.19 g, 10.0 mmol), polymer supported triphenylphosphine (9.3 g, 20.0 mmol), and *trans*-cyclohexane-1,4-dimethanol (2.88 g, 20.0 mmol) in THF (200 mL) cooled to 0 °C. The mixture was allowed to warm to rt. After 18 h, the reaction mixture was filtered, and the resin was washed with THF (100 mL). The filtrate was concentrated. The residue was dissolved in EtOAc (200 mL) and washed with water (50 mL). The organic layer was dried (Na<sub>2</sub>SO<sub>4</sub>) and concentrated. The crude product was purified by silica column chromatography (CH<sub>2</sub>Cl<sub>2</sub>/methanol, 100/1–100/4) to afford 2.3 g (67%) of **32** as an oil. <sup>1</sup>H NMR (400 MHz, DMSO-*d*<sub>6</sub>) δ 8.40 (d, *J* = 0.8 Hz, 1 H), 8.12 (d, *J* = 1.1 Hz, 1 H), 4.67 (d, *J* = 7.0 Hz, 2 H), 4.35 (t, *J* = 5.3 Hz, 1 H), 3.93 (s, 3 H), 3.19 (t, *J* = 5.8 Hz, 2 H), 2.66 (s, 3 H), 2.04–1.90 (m, 1 H), 1.74 (d, *J* = 10.6 Hz, 2 H), 1.61 (d, *J* = 10.6 Hz, 2 H), 1.37–1.23 (m, 1 H), 1.08 (dq, *J* = 12.6, 2.7 Hz, 2 H), 0.87 (dq, *J* = 12.8, 3.1 Hz, 2 H). MS (ES+) *m/z* 346 (M + H).

**4-(2-(((*trans*)-4-(Hydroxymethyl)cyclohexyl)methyl)-2H-tetrazol-5-yl)-6-methylpicolinic Acid (33)**. Lithium hydroxide (479 mg, 20.0 mmol) was added to a solution of **32** (2.3 g, 6.68 mmol) dissolved in a mixture of THF/water (40 mL, 1/1), and the mixture was stirred at rt for 3 h. The solvent was removed in vacuo, and the residue was diluted with water (20 mL). The solution was made acidic with 1 N HCl solution (20 mL), and the resulting precipitate was filtered to afford 1.03 g (47%) of **33** as a white solid. <sup>1</sup>H NMR (400 MHz, DMSO-*d*<sub>6</sub>) δ 13.36 (br, 1 H), 8.40 (d, *J* = 0.8 Hz, 1 H), 8.09 (d, *J* = 1.1 Hz, 1 H), 4.66 (d, *J* = 7.1 Hz, 2 H), 4.35 (br. s., 1 H), 3.19 (d, *J* = 6.2 Hz, 2 H), 2.65 (s, 3 H), 2.03–1.90 (m, 1 H), 1.74 (d, *J* = 10.5 Hz, 2 H), 1.61 (d, *J* = 10.9, 2 H), 1.35–1.25 (m, 1 H), 1.08 (dq, *J* = 12.6, 2.8 Hz, 2 H), 0.87 (dq, *J* = 12.8, 3.2 Hz, 2 H). MS (ES+) *m/z* 332 (M + H).

**General Procedure for Synthesis of Amides 34a–I**. A mixture of **33** (33 mg, 0.10 mmol) and 1-hydroxybenzotriazole (18.9 mg, 0.14 mmol) in DMF (0.5 mL) was shaken for 15 min. *N*-Methylmorpholine (44 μL, 0.40 mmol) was added followed by the corresponding benzylamine (0.12 mmol) in DMF (0.5 mL). 1-Ethyl-3-(3'-dimethylaminopropyl)carbodiimide hydrochloride (26.8 mg, 0.14 mmol) was then added, and the mixture was shaken for 18 h. The reaction mixture was purified by reverse phase preparative HPLC to afford the title compound.

**N-Benzyl-4-(2-(((*trans*)-4-(hydroxymethyl)cyclohexyl)methyl)-2H-tetrazol-5-yl)-6-methylpicolinamide (34a)**. 76% yield. <sup>1</sup>H NMR (400 MHz, DMSO-*d*<sub>6</sub>) δ 9.26 (t, *J* = 6.4 Hz, 1 H), 8.39 (s, 1 H), 8.04 (s, 1 H), 7.18–7.35 (m, 5 H), 4.62 (d, *J* = 7.0, 2 H), 4.50 (d, *J* = 6.2 Hz, 2 H), 4.32 (t, *J* = 5.3 Hz, 1 H), 3.14 (t, *J* = 5.9 Hz, 2 H), 2.63 (s, 3 H), 1.99–1.86 (m, 1 H), 1.70 (d, *J* = 11.7 Hz, 2 H), 1.57 (d, *J* = 12.1 Hz, 2 H), 1.32–1.20 (m, 1 H), 1.03 (q, *J* = 12.0 Hz, 2 H), 0.83 (q, *J* = 12.0 Hz, 2 H). MS (ES+) *m/z* 421 (M + H).

**N-(4-Fluorobenzyl)-4-(2-(((*trans*)-4-(hydroxymethyl)cyclohexyl)methyl)-2H-tetrazol-5-yl)-6-methylpicolinamide (34b)**. 52% yield. <sup>1</sup>H NMR (400 MHz, DMSO-*d*<sub>6</sub>) δ 9.35 (t, *J* = 6.4 Hz, 1 H), 8.43 (s, 1 H), 8.09 (s, 1 H), 7.39 (dd, *J* = 8.4, 5.7 Hz, 2 H), 7.16 (t, *J* = 8.9 Hz, 2 H), 4.67 (d, *J* = 7.0 Hz, 2 H), 4.52 (d, *J* = 6.3 Hz, 2 H), 4.37 (t, *J* = 5.3 Hz, 1 H), 3.19 (t, *J* = 5.7 Hz, 2 H), 2.68 (s, 3 H), 1.91–2.02 (m, 1 H), 1.71–1.78 (m, 2 H), 1.58–1.64 (m, 2 H), 1.24–1.37 (m, 1 H), 1.02–1.14 (m, 2 H), 0.81–0.94 (m, 2 H). MS (ES+) *m/z* 439 (M + H).

**N-(3-Fluorobenzyl)-4-(2-(((*trans*)-4-(hydroxymethyl)cyclohexyl)methyl)-2H-tetrazol-5-yl)-6-methylpicolinamide (34c)**. 20% yield. <sup>1</sup>H NMR (400 MHz, DMSO-*d*<sub>6</sub>) δ 9.37 (t, *J* = 6.4 Hz, 1 H), 8.43 (d, *J* = 0.9 Hz, 1 H), 8.09 (d, *J* = 1.1 Hz, 1 H), 7.40–7.34 (m, 1 H), 7.21–7.13 (m, 2 H), 7.07 (dt, *J* = 8.5, 2.4 Hz, 1 H), 4.66 (d, *J* = 6.9 Hz, 2 H), 4.55 (d, *J* = 6.4 Hz, 2 H), 4.35 (t, *J* = 5.3 Hz, 1 H), 3.19 (t, *J* = 5.8 Hz, 2 H), 2.66 (s, 3

H), 2.04–1.91 (m, 1 H), 1.74 (d,  $J = 11.0$  Hz, 2 H), 1.62 (d,  $J = 12.0$  Hz, 2 H), 1.35–1.25 (m, 1 H), 1.08 (q,  $J = 13.2$  Hz, 2 H), 0.87 (q,  $J = 11.2$  Hz, 2 H). MS (ES+)  $m/z$  439 (M + H).

***N*-(3-Chlorobenzyl)-4-(2-(((trans)-4-(hydroxymethyl)cyclohexyl)methyl)-2H-tetrazol-5-yl)-6-methylpicolinamide (34d)**. 35% yield.  $^1\text{H}$  NMR (400 MHz, DMSO- $d_6$ )  $\delta$  9.37 (t,  $J = 6.4$  Hz, 1 H), 8.38 (s, 1 H), 8.05 (s, 1 H), 7.26–7.37 (m, 4 H), 4.62 (d,  $J = 7.0$  Hz, 2 H), 4.49 (d,  $J = 6.6$  Hz, 2 H), 4.33 (t,  $J = 5.3$  Hz, 1 H), 3.14 (t,  $J = 5.7$  Hz, 2 H), 2.64 (s, 3 H), 1.97–1.87 (m, 1 H), 1.70 (d,  $J = 10.6$  Hz, 2 H), 1.57 (d,  $J = 11.3$  Hz, 2 H), 1.31–1.21 (m, 1 H), 1.03 (q,  $J = 12.4$  Hz, 2 H), 0.83 (q,  $J = 12.4$  Hz, 2 H). MS (ES+)  $m/z$  455 (M + H).

***N*-(3-Methylbenzyl)-4-(2-(((trans)-4-(hydroxymethyl)cyclohexyl)methyl)-2H-tetrazol-5-yl)-6-methylpicolinamide (34e)**. 77% yield.  $^1\text{H}$  NMR (400 MHz, DMSO- $d_6$ )  $\delta$  9.21 (t,  $J = 6.4$  Hz, 1 H), 8.39 (s, 1 H), 8.04 (s, 1 H), 7.17 (t,  $J = 7.5$  Hz, 1 H), 7.07–7.13 (m, 2 H), 7.02 (d,  $J = 7.3$  Hz, 1 H), 4.62 (d,  $J = 7.0$  Hz, 2 H), 4.46 (d,  $J = 6.2$  Hz, 2 H), 4.32 (t,  $J = 5.1$  Hz, 1 H), 3.14 (t,  $J = 5.9$  Hz, 2 H), 2.63 (s, 3 H), 2.24 (s, 3 H), 1.97–1.87 (m, 1 H), 1.70 (d,  $J = 11.0$  Hz, 2 H), 1.57 (d,  $J = 11.3$  Hz, 2 H), 1.30–1.20 (m, 1 H), 1.04 (q,  $J = 13.2$  Hz, 2 H), 0.83 (q,  $J = 12.2$  Hz, 2 H). MS (ES+)  $m/z$  435 (M + H).

***N*-(3-(Trifluoromethyl)benzyl)-4-(2-(((trans)-4-(hydroxymethyl)cyclohexyl)methyl)-2H-tetrazol-5-yl)-6-methylpicolinamide (34f)**. 77% yield.  $^1\text{H}$  NMR (400 MHz, DMSO- $d_6$ )  $\delta$  9.43 (t,  $J = 6.2$  Hz, 1 H), 8.37 (s, 1 H), 8.04 (s, 1 H), 7.69–7.48 (m, 4 H), 4.61 (d,  $J = 7.0$  Hz, 2 H), 4.56 (d,  $J = 6.2$  Hz, 2 H), 4.31 (t,  $J = 5.1$  Hz, 1 H), 3.13 (t,  $J = 5.7$  Hz, 2 H), 2.63 (s, 3 H), 1.98–1.85 (m, 1 H), 1.68 (d,  $J = 11.7$  Hz, 2 H), 1.56 (d,  $J = 11.3$  Hz, 2 H), 1.31–1.19 (m, 1 H), 1.02 (q,  $J = 12.8$  Hz, 2 H), 0.82 (q,  $J = 12.4$  Hz, 2 H). MS (ES+)  $m/z$  489 (M + H).

***N*-(3,4-Difluorobenzyl)-4-(2-(((trans)-4-(hydroxymethyl)cyclohexyl)methyl)-2H-tetrazol-5-yl)-6-methylpicolinamide (34g)**. 74% yield.  $^1\text{H}$  NMR (400 MHz, DMSO- $d_6$ )  $\delta$  9.36 (t,  $J = 6.4$  Hz, 1 H), 8.38 (s, 1 H), 8.05 (s, 1 H), 7.39–7.30 (m, 2 H), 7.13–7.18 (m, 1 H), 4.62 (d,  $J = 7.0$  Hz, 2 H), 4.47 (d,  $J = 6.6$  Hz, 2 H), 4.32 (t,  $J = 5.3$  Hz, 1 H), 3.14 (t,  $J = 5.9$  Hz, 2 H), 2.64 (s, 3 H), 1.97–1.87 (m, 1 H), 1.70 (d,  $J = 11.0$  Hz, 2 H), 1.57 (d,  $J = 12.1$  Hz, 2 H), 1.30–1.18 (m, 1 H), 1.03 (q,  $J = 12.8$  Hz, 2 H), 0.83 (q,  $J = 11.3$  Hz, 2 H). MS (ES+)  $m/z$  457 (M + H).

***N*-(3-Chloro-4-fluorobenzyl)-4-(2-(((trans)-4-(hydroxymethyl)cyclohexyl)methyl)-2H-tetrazol-5-yl)-6-methylpicolinamide (34h)**. 53% yield.  $^1\text{H}$  NMR (400 MHz, DMSO- $d_6$ )  $\delta$  9.40 (t,  $J = 8.4$  Hz, 1 H), 8.42 (d,  $J = 0.9$  Hz, 1 H), 8.09 (d,  $J = 1.2$  Hz, 1 H), 7.56 (d,  $J = 7.7$  Hz, 1 H), 7.39–7.35 (m, 2 H), 4.66 (d,  $J = 7.1$  Hz, 2 H), 4.51 (d,  $J = 6.4$  Hz, 2 H), 4.35 (t,  $J = 5.3$  Hz, 1 H), 3.19 (t,  $J = 5.8$  Hz, 2 H), 2.68 (s, 3 H), 2.03–1.90 (m, 1 H), 1.74 (d,  $J = 10.6$  Hz, 2 H), 1.61 (d,  $J = 10.7$  Hz, 2 H), 1.35–1.24 (m, 1 H), 1.08 (dq,  $J = 12.4$ , 2.4 Hz, 2 H), 0.87 (dq,  $J = 12.6$ , 3.0 Hz, 2 H). MS (ES+)  $m/z$  473 (M + H).

***N*-(4-Fluoro-3-methylbenzyl)-4-(2-(((trans)-4-(hydroxymethyl)cyclohexyl)methyl)-2H-tetrazol-5-yl)-6-methylpicolinamide (34i)**. 79% yield.  $^1\text{H}$  NMR (400 MHz, DMSO- $d_6$ )  $\delta$  9.25 (t,  $J = 6.2$  Hz, 1 H), 8.38 (s, 1 H), 8.04 (s, 1 H), 7.21 (d,  $J = 7.3$  Hz, 1 H), 7.17–7.13 (m, 1 H), 7.03 (t,  $J = 9.2$  Hz, 1 H), 4.62 (d,  $J = 7.0$  Hz, 2 H), 4.43 (d,  $J = 6.2$  Hz, 2 H), 4.32 (t,  $J = 5.1$  Hz, 1 H), 3.14 (t,  $J = 5.7$  Hz, 2 H), 2.63 (s, 3 H), 2.17 (s, 3 H), 1.97–1.87 (m, 1 H), 1.70 (d,  $J = 11.0$  Hz, 2 H), 1.57 (d,  $J = 13.2$  Hz, 2 H), 1.30–1.20 (m, 1 H), 1.03 (q,  $J = 10.6$  Hz, 2 H), 0.83 (q,  $J = 12.4$  Hz, 2 H). MS (ES+)  $m/z$  453 (M + H).

***N*-(4-Fluoro-3-(trifluoromethyl)benzyl)-4-(2-(((trans)-4-(hydroxymethyl)cyclohexyl)methyl)-2H-tetrazol-5-yl)-6-methylpicolinamide (34j)**. 59% yield.  $^1\text{H}$  NMR (400 MHz, DMSO- $d_6$ )  $\delta$  9.43 (t,  $J = 6.2$  Hz, 1 H), 8.37 (s, 1 H), 8.05 (s, 1 H), 7.73 (d,  $J = 6.2$  Hz, 1 H), 7.71–7.66 (m, 1 H), 7.47–7.40 (m, 1 H), 4.62 (d,  $J = 7.0$  Hz, 2 H), 4.53 (d,  $J = 6.2$  Hz, 2 H), 4.32 (t,  $J = 5.3$  Hz, 1 H), 3.14 (t,  $J = 5.5$  Hz, 2 H), 2.64 (s, 3 H), 1.97–1.87 (m, 1 H), 1.69 (d,  $J = 10.6$  Hz, 2 H), 1.57 (d,  $J = 11.3$  Hz, 2 H), 1.30–1.20 (m, 1 H), 1.03 (q,  $J = 12.8$  Hz, 2 H), 0.83 (q,  $J = 12.4$  Hz, 2 H). MS (ES+)  $m/z$  507 (M + H).

***N*-(4-Fluoro-3-methoxybenzyl)-4-(2-(((trans)-4-(hydroxymethyl)cyclohexyl)methyl)-2H-tetrazol-5-yl)-6-methylpicolinamide (34k)**. 28% yield.  $^1\text{H}$  NMR (400 MHz, CDCl $_3$ )  $\delta$  8.70 (s, 1 H), 8.42 (t,  $J = 6.2$  Hz, 1 H), 8.03 (d,  $J = 1.3$  Hz, 1 H), 7.06–6.94 (m, 2 H), 6.92–6.85 (m, 1 H), 4.62 (d,  $J = 6.4$  Hz, 2 H), 4.52 (d,  $J = 7.0$  Hz, 2 H), 3.86 (s, 3 H), 3.48–3.38 (m, 3 H), 2.61 (s, 3 H), 2.14–2.00 (m, 1 H), 1.90–1.66

(m, 4 H), 1.54–1.39 (m, 1 H), 1.19–1.05 (m, 2 H), 1.04–0.91 (m, 2 H). 99% MS (ES+)  $m/z$  469 (M + H).

**6-Chloro-2-methylpyrimidin-4-ol (36)**. 4,6-Dichloro-2-methylpyrimidine 35 (475 g, 2.91 mol) was added portionwise to a solution of 13 M sulfuric acid (1.2 L, 15.6 mol) at 0 °C. The resulting mixture was allowed to warm to rt over 1.5 h. The solution was poured into a well stirred mixture of ice and 6 N NaOH (3.6 L, 21.6 mol). The resulting solids were then collected by vacuum filtration, washed with warm water (3  $\times$  1 L), and dried at 35 °C under high vacuum to provide 393.4 g (93%) of 36 as a white solid.  $^1\text{H}$  NMR (400 MHz, DMSO- $d_6$ )  $\delta$  12.81 (br. s, 1 H), 6.30 (s, 1 H), 2.26 (s, 3 H). MS (ES+)  $m/z$  145 (M + H).

**Methyl 6-Hydroxy-2-methylpyrimidine-4-carboxylate (37)**. A solution of 36 (36.7 g, 254 mmol), [1,1'-bis(diphenylphosphino)ferrocene]palladium(II) dichloride (10.4 g, 12.7 mmol), and diisopropylethylamine (49.2 g, 381 mmol) in methanol (254 mL) was heated at 85 °C in the presence of carbon monoxide (50 psi) for 24 h. The reaction mixture was allowed to cool to rt. The resulting solids were collected by vacuum filtration, rinsed with methanol (100 mL) followed by diethyl ether (2  $\times$  100 mL), and dried under vacuum to provide 38.7 g (91%) of 37 as a brown solid.  $^1\text{H}$  NMR (400 MHz, DMSO- $d_6$ )  $\delta$  12.79 (br. s, 1 H), 6.68 (s, 1 H), 3.79 (s, 3 H), 2.29 (s, 3 H). MS (ES+)  $m/z$  169 (M + H).

**Methyl 6-Chloro-2-methylpyrimidine-4-carboxylate (38)**. Oxalyl chloride (18.6 mL, 213 mmol) and DMA (3.5 mL, 44 mmol) were added to a solution of 37 (30.0 g, 178 mmol) in dichloromethane (446 mL). The mixture was heated at reflux for 2 h. After cooling to rt, the mixture was filtered. The filtrate was partially concentrated and purified by silica gel chromatography (35/65, EtOAc/heptane) to provide 26.6 g (80%) of 38 as a white solid.  $^1\text{H}$  NMR (400 MHz, DMSO- $d_6$ )  $\delta$  7.90 (s, 1 H), 3.88 (s, 3 H), 2.65 (s, 3 H). MS (ES+)  $m/z$  187 (M + H).

**Methyl 6-Cyano-2-methylpyrimidine-4-carboxylate (39)**. Tetraethylammonium cyanide (27.6 g, 177 mmol) and DABCO (3.60 g, 32.0 mmol) was added to a solution of 38 (30.0 g, 161 mmol) in dichloromethane (460 mL), and the mixture was stirred for 30 min at rt. The reaction mixture was washed with 1 N NaOH (3  $\times$  100 mL), water (2  $\times$  100 mL), and brine (200 mL). The organic layer was dried (Na $_2$ SO $_4$ ), filtered, and concentrated. The crude product was purified by silica gel chromatography (2/1, EtOAc/heptane) to provide 24.4 g (86%) of 39 as a white crystalline solid.  $^1\text{H}$  NMR (400 MHz, DMSO- $d_6$ )  $\delta$  8.38 (s, 1 H), 3.88 (s, 3 H), 2.75 (s, 3 H). MS (ES+)  $m/z$  178 (M + H).

**6-Cyano-*N*-(3-methoxybenzyl)-2-methylpyrimidine-4-carboxamide (40a)**. Diisopropylethylamine (25.5 g, 198 mmol) was added to a solution of 3-methoxybenzylamine (9.68 g, 70.6 mmol) and 39 (10.0 g, 56.4 mmol) in DMA (113 mL), and the mixture was heated at 100 °C for 2 h. After cooling to rt, the mixture was diluted with water (250 mL) and extracted with EtOAc (3  $\times$  250 mL). The combined organic layers were washed with brine (250 mL), dried (NaSO $_4$ ), filtered, and concentrated. The crude product was purified by silica gel chromatography (20/80, EtOAc/heptane) to provide 14.6 g (92%) of 40a as a white solid.  $^1\text{H}$  NMR (400 MHz, DMSO- $d_6$ )  $\delta$  9.55 (t,  $J = 6.2$  Hz, 1 H), 8.31 (s, 1 H), 7.19 (t,  $J = 8.1$  Hz, 1 H), 6.74–6.89 (m, 3 H), 4.44 (d,  $J = 6.3$  Hz, 2 H), 3.69 (s, 3 H), 2.75 (s, 3 H). MS (ES+)  $m/z$  283 (M + H).

**6-Cyano-*N*-(4-fluoro-3-methoxybenzyl)-2-methylpyrimidine-4-carboxamide (40b)**. A mixture of 4-fluoro-3-methoxybenzylamine hydrochloride (13.5 g, 70.6 mmol) and diisopropylethylamine (29.2 g, 226 mmol) in methanol (56 mL) was stirred for 15 min at rt. Compound 39 (10.0 g, 56.4 mmol) was added, and the reaction mixture was heated at 35 °C for 1 h. The methanol was removed in vacuo, and the residue was partitioned between EtOAc (500 mL) and 1 N HCl (500 mL). The aqueous layer was extracted with EtOAc (2  $\times$  250 mL). The combined organic layers were washed with saturated aqueous sodium bicarbonate (2  $\times$  250 mL) followed by brine (250 mL), dried (Na $_2$ SO $_4$ ), filtered, and concentrated. The crude product was purified by silica gel chromatography (1/2, EtOAc/heptane) to provide 11.7 g (69%) of 40b as a white solid.  $^1\text{H}$  NMR (400 MHz, DMSO- $d_6$ )  $\delta$  9.58 (t,  $J = 6.2$  Hz, 1 H), 8.32 (s, 1 H), 7.04–7.19 (m, 2 H), 6.79–6.90 (m, 1 H), 4.44 (d,  $J = 6.2$  Hz, 2 H), 3.78 (s, 3 H), 2.76 (s, 3 H). MS (ES+)  $m/z$  301 (M + H).

***N*-(3-Methoxybenzyl)-2-methyl-6-(2H-tetrazol-5-yl)pyrimidine-4-carboxamide (41a)**. A suspension of 40a (14.2 g, 50.3

mmol), sodium azide (3.60 g, 55.3 mmol), and zinc bromide (11.3 g, 50.3 mmol) in water (112 mL) was heated at reflux for 16 h. **CAUTION!** *Solvent represents an explosion hazard at elevated temperatures. Adequate blast shielding is recommended.* After the mixture cooled to rt, 6 N HCl (180 mL) was added, and the mixture was stirred vigorously for 1 h. The resulting solids were collected by vacuum filtration, rinsed with 6 N HCl (3 × 100 mL) followed by water (2 × 100 mL), and dried at 55 °C under vacuum to provide 15.0 g (92%) of **40a** as a white solid. <sup>1</sup>H NMR (400 MHz, DMSO-*d*<sub>6</sub>) δ 9.53 (t, *J* = 6.4 Hz, 1 H), 8.42 (s, 1 H), 7.21 (t, *J* = 8.2 Hz, 1 H), 6.86–6.91 (m, 2 H), 6.76–6.82 (m, 1 H), 4.48 (d, *J* = 6.6 Hz, 2 H), 3.70 (s, 3 H), 2.82 (s, 3 H). MS (ES+) *m/z* 326 (M + H).

**N-(4-Fluoro-3-methoxybenzyl)-2-methyl-6-(2H-tetrazol-5-yl)pyrimidine-4-carboxamide (41b).** Following conditions analogous to those described for **41a**, reaction of **40b** (4.80 g, 16.0 mmol) provided 5.45 g (99%) of **41b** as a white solid. <sup>1</sup>H NMR (400 MHz, DMSO-*d*<sub>6</sub>) δ 9.55 (t, *J* = 6.4 Hz, 1 H), 8.42 (s, 1 H), 7.06–7.20 (m, 2 H), 6.81–6.94 (m, 1 H), 4.47 (d, *J* = 6.4 Hz, 2 H), 3.79 (s, 3 H), 2.82 (s, 3 H). MS (ES+) *m/z* 344 (M + H).

**rac-N-(3-Methoxybenzyl)-6-(2-(((2*S*\*,5*R*\*)-5-(hydroxymethyl)-1,4-dioxan-2-yl)methyl)-2H-tetrazol-5-yl)-2-methylpyrimidine-4-carboxamide (42).** A mixture of *rac*-**16** (4.3 g, 14.0 mmol), **41a** (3.2 g, 9.8 mmol), and triethylamine (2.0 g, 19.7 mmol) in anhydrous DMA (4 mL) was heated at 85 °C for 18 h. The reaction mixture was purified by reverse phase preparative HPLC to afford 1.38 g (31%) of **42** as a white solid. <sup>1</sup>H NMR (400 MHz, DMSO-*d*<sub>6</sub>) δ 9.52–9.44 (m, 1 H), 8.42 (s, 1 H), 7.24 (t, *J* = 8.1 Hz, 1 H), 6.95–6.89 (m, 2 H), 6.83 (d, *J* = 8.1 Hz, 1 H), 4.93 (d, *J* = 3.3 Hz, 1 H), 4.88 (d, *J* = 7.7 Hz, 1 H), 4.51 (d, *J* = 5.9 Hz, 3 H), 4.08 (d, *J* = 3.3 Hz, 1 H), 3.99 (d, *J* = 11.3 Hz, 1 H), 3.78 (d, *J* = 11.3 Hz, 1 H), 3.74 (s, 3 H), 3.48–3.36 (m, 4 H), 3.31 (d, *J* = 2.2 Hz, 1H), 2.83 (s, 3 H). MS (ES+) *m/z* 456 (M + H).

**N-(4-Fluoro-3-methoxybenzyl)-6-(2-(((2*S*,5*R*)-5-(hydroxymethyl)-1,4-dioxan-2-yl)methyl)-2H-tetrazol-5-yl)-2-methylpyrimidine-4-carboxamide (43a).** A mixture of **(2*R*,5*R*)-16** (12.4 g, 41.0 mmol), **41b** (10.0 g, 29.1 mmol), and triethylamine (7.04 g, 69.7 mmol) in anhydrous DMA (31 mL) was heated at 85 °C for 18 h. After cooling to rt, the mixture was diluted with water (300 mL) and extracted with dichloromethane (3 × 200 mL). The combined organic layers were washed with 1 N NaOH (2 × 100 mL), 1 M HCl (2 × 100 mL), water (100 mL), and brine (250 mL). The organic layer was dried (Na<sub>2</sub>SO<sub>4</sub>), filtered, and evaporated. The residue was purified by silica gel chromatography (heptane/EtOAc/methanol, 50/45/5). The resulting mixture of regioisomers was separated by SFC (OJ-H, 30 mm × 250 mm, 40% methanol, 70 mL/min), and the desired isomer was recrystallized from EtOAc/ethanol (80/1, 80 mL) to provide 3.5 g (25%) of **43a** as a white solid. <sup>1</sup>H NMR (400 MHz, DMSO-*d*<sub>6</sub>) δ 9.53 (t, *J* = 6.3 Hz, 1 H), 8.39 (s, 1 H), 7.19–7.06 (m, 2 H), 6.91–6.83 (m, 1 H), 4.98–4.78 (m, 2 H), 4.68 (t, *J* = 5.7 Hz, 1 H), 4.47 (d, *J* = 6.4 Hz, 2 H), 4.10–3.99 (m, 1 H), 3.96 (dd, *J* = 11.4, 2.4 Hz, 1 H), 3.79 (s, 3 H), 3.74 (dd, *J* = 11.4, 2.2 Hz, 1 H), 3.47–3.19 (m, 5 H), 2.80 (s, 3 H). MS (ES+) *m/z* 474 (M + H).

**N-(4-Fluoro-3-methoxybenzyl)-6-(2-(((2*R*,5*S*)-5-(hydroxymethyl)-1,4-dioxan-2-yl)methyl)-2H-tetrazol-5-yl)-2-methylpyrimidine-4-carboxamide (43b).** Analogous to the procedures for **43a**, **(2*S*,5*S*)-16** (5.2 g, 17.2 mmol) was reacted with **41b** (4.22 g, 12.3 mmol). The minor regioisomer was removed by SFC (OJ-H, 30 mm × 250 mm, 45% acetonitrile, 70 mL/min), and the desired isomer was recrystallized from EtOAc to afford 1.5 g (26%) of **43b** as a white solid. <sup>1</sup>H NMR (400 MHz, DMSO-*d*<sub>6</sub>) δ 9.50 (t, *J* = 6.2 Hz, 1 H), 8.42 (s, 1 H), 7.17–7.08 (m, 2 H), 6.90–6.85 (m, 1 H), 4.95–4.80 (m, 2 H), 4.69 (t, *J* = 5.5 Hz, 1 H), 4.47 (d, *J* = 6.2 Hz, 2 H), 4.09–3.93 (m, 2 H), 3.79 (s, 3 H), 3.77–3.71 (m, 1 H), 3.45–3.20 (m, 5 H), 2.79 (s, 3 H). MS (ES+) *m/z* 474 (M + H).

**(2*S*,5*S*)-5-((5-(6-((4-Fluoro-3-methoxybenzyl)carbamoyl)-2-methylpyrimidin-4-yl)-2H-tetrazol-2-yl)methyl)-1,4-dioxane-2-carboxylic acid (45).** A mixture of **43a** (952 mg, 2.0 mmol) and pyridinium dichromate (4.61 g, 12.0 mmol) in DMF (20.0 mL) was shaken for 36 h at rt. The reaction mixture was poured into EtOAc (250 mL) and washed with 1 N HCl solution (2 × 50 mL). The organic layer was dried (Na<sub>2</sub>SO<sub>4</sub>) and concentrated. The residue was suspended in 1 N sodium hydroxide solution and extracted with EtOAc. The aqueous layer was acidified to pH 2 with concentrated HCl and extracted with

dichloromethane. The combined organic layers were dried (Na<sub>2</sub>SO<sub>4</sub>) and concentrated. The resulting oil was purified by reverse phase HPLC. The acetonitrile was removed in vacuo, and the aqueous residue was extracted with dichloromethane (2 × 50 mL). The combined organic layers were concentrated. The crude product was triturated with ethyl ether (3×) to afford 361 mg (37%) of **45** as a white solid. <sup>1</sup>H NMR (400 MHz, DMSO-*d*<sub>6</sub>) 13.03 (s, 1 H), 9.58 (t, *J* = 6.4 Hz, 1 H), 8.42 (s, 1 H), 7.21–7.17 (m, *J* = 8.5, 1.5 Hz, 1 H), 7.18–7.11 (dd, *J* = 11.6, 8.4 Hz, 1 H), 6.93–6.88 (m, 1 H), 4.98 (dd, *J* = 14.3, 3.8 Hz, 1 H), 4.91 (dd, *J* = 14.2, 7.9 Hz, 1 H), 4.50 (d, *J* = 6.3 Hz, 2 H), 4.17–4.05 (m, 3 H), 3.95 (dd, *J* = 11.8, 2.9 Hz, 1 H), 3.82 (s, 3 H), 3.49 (dt, *J* = 18.1, 10.8 Hz, 2 H), 2.83 (s, 3 H). MS (ES+) *m/z* 488 (M + H).

**Collagenase Activity.** Apparent inhibition constants (*K*<sub>i,app</sub>) were determined using the synthetic quenched fluorescent peptide substrate MCA-Arg-Pro-Leu-Gly-Leu-Dpa-Ala-Arg-Glu-Arg-NH<sub>2</sub> as previously described.<sup>29</sup> Full-length recombinant human proteins were used for MMPs 1, 2, 9, and 13. The catalytic domain of the protein was used for MMPs 3, 7, 8, 10, 12, 14, 15, 16, 20, 24, 25, and 26. Selectivity against ADAM-17 (TACE), ADAMTS-4 (aggrecanase 1), and ADAMTS-5 (aggrecanase 2) was determined as previously described.<sup>29</sup>

**In Vivo Animal Studies.** All procedures performed on animals were in accordance with regulations and established guidelines and were reviewed and approved by Pfizer Institutional Animal Care and Use Committee.

For determination of rat in vivo clearance, each test compound was dissolved in 70% PEG400/10% ethanol/20% normal saline vehicle at 0.5 mg/mL and dosed at 2 mL/kg via IV bolus to *N* = 2 male Sprague–Dawley IGS rats weighing 250–300 g. Blood was collected over a 24 h time course, and following centrifugation the resulting plasma samples were precipitated with acetonitrile and analyzed for test compound concentration using an LC-MS/MS procedure. PK parameters were calculated from plasma concentration–time curves using noncompartmental analysis in Watson LIMS. For cassette dose PK, the procedure was identical except five compounds were dissolved in vehicle at 0.1 mg/mL each and dosed simultaneously, resulting in a combined total dose by mass that was the same as for singleton PK.

For dog PK, test compounds were dosed orally as a suspension in 0.5% Methocel/0.1% TWEEN80 to fasted male beagle dogs. Compounds were dosed at 5 mL/kg by gavage in a cassette experiment (*N* = 5/cassette) such that each animal received a dose equivalent to 1.0 mg/kg of each compound in a single experiment. Blood collection, sample processing, concentration determination, and PK calculations were identical to the procedure used for rat PK.

In cynomolgus monkeys, compound **43a** was administered once daily by oral gavage using a 50% drug load spray-dried dispersion formulation in a 50% by weight aqueous sucrose solution. Doses of 50, 100, and 1000 mg kg<sup>-1</sup> day<sup>-1</sup> were administered for 14 days (one male and one female per dose group). Gross necropsy observations, clinical pathology, and histopathology of the kidneys were evaluated.

## ■ ASSOCIATED CONTENT

### 📄 Supporting Information

The Supporting Information is available free of charge on the ACS Publications website at DOI: 10.1021/acs.jmedchem.5b01434.

Synthesis and X-ray data collection for the crystal structure of compound **44** and pharmacokinetic parameters of compounds **14i**, **42**, and **43b** in rat and compound **43a** in rat, dog, and cynomolgus monkey.(PDF)

SMILES representations of compounds with MMP13/FL K<sub>i</sub> (XLSX)

## ■ AUTHOR INFORMATION

### Corresponding Author

\*Phone: 617-674-7362. E-mail: mark.e.schnute@pfizer.com.

### Notes

The authors declare no competing financial interest.

## ACKNOWLEDGMENTS

We thank Jon Bordner for single crystal X-ray data collection, members of Pfizer pharmacokinetics and drug metabolism group for in vivo exposure and metabolite characterization, and members of Pfizer drug safety group for in vivo toxicology support.

## ABBREVIATIONS

AUC, area under the curve; CD, catalytic domain; CL, clearance; %F, bioavailability (fraction bioavailable); DABCO, 1,4-diazabicyclo[2.2.2]octane; DBAD, di-*tert*-butyl azodicarboxylate; DCE, dichloroethane; DMA, *N,N*-dimethylacetamide; DMAP, 4-(dimethylamino)pyridine; DMF, *N,N*-dimethylformamide; DMSO, dimethyl sulfoxide; dppf, 1,1'-bis-(diphenylphosphino)ferrocene; EDCI, 1-ethyl-3-(3'-dimethylaminopropyl)carbodiimide hydrochloride; EtOAc, ethyl acetate; FL, full length; HLM, human liver microsomes; HPLC, high-pressure liquid chromatography; LC-MS/MS, liquid chromatography-tandem mass spectrometry; LIPE, lipophilic ligand efficiency; MMP, matrix metalloproteinase; PPB, plasma protein binding; rt, room temperature; SAR, structure-activity relationships; SFC, supercritical fluid chromatography;  $T_{1/2}$ , half-life; TFA, trifluoroacetic acid; THF, tetrahydrofuran

## REFERENCES

- (1) Lawrence, R. C.; Felson, D. T.; Helmick, C. G.; Arnold, L. M.; Choi, H.; Deyo, R. A.; Gabriel, S.; Hirsch, R.; Hochberg, M. C.; Hunder, G. C.; Jordan, J. M.; Katz, J. N.; Kremers, H. M.; Wolfe, F. Estimates of the prevalence of arthritis and other rheumatic conditions in the United States. Part II. *Arthritis Rheum.* **2008**, *58*, 26–35.
- (2) Johnson, V. L.; Hunter, D. J. The epidemiology of osteoarthritis. *Best Pract. Res. Clin. Rheumatol.* **2014**, *28*, 5–15.
- (3) Felson, D. T. Osteoarthritis of the Knee. *N. Engl. J. Med.* **2006**, *354*, 841–848.
- (4) Hellio le Graverand, M.-P.; Clemmer, R. S.; Redifer, P.; Brunell, R. M.; Hayes, C. W.; Brandt, K. D.; Abramson, S. B.; Manning, P. M.; Miller, C. G.; Vignon, E. A 2-year randomised, double-blind, placebo-controlled, multicentre study of oral selective iNOS inhibitor, cindunistat (SD-6010), in patients with symptomatic osteoarthritis of the knee. *Ann. Rheum. Dis.* **2013**, *72*, 187–195.
- (5) Little, C. B.; Barai, A.; Burkhardt, D.; Smith, S. M.; Fosang, A. J.; Werb, Z.; Shah, M.; Thompson, E. W. Matrix metalloproteinase 13-deficient mice are resistant to osteoarthritic cartilage erosion but not chondrocyte hypertrophy or osteophyte development. *Arthritis Rheum.* **2009**, *60*, 3723–3733.
- (6) Johnson, A. R.; Pavlovsky, A. G.; Ortwine, D. F.; Prior, F.; Man, C.-F.; Bornemeier, D. A.; Banotai, C. A.; Mueller, W. T.; McConnell, P.; Yan, C.; Baragi, V.; Lesch, C.; Roark, W. H.; Wilson, M.; Datta, K.; Guzman, R.; Han, H.-K.; Dyer, R. D. Discovery and characterization of a novel inhibitor of matrix metalloproteinase-13 that reduces cartilage damage in vivo without joint fibroplasia side effects. *J. Biol. Chem.* **2007**, *282*, 27781–27791.
- (7) Baragi, V. M.; Becher, G.; Bendele, A. M.; Biesinger, R.; Bluhm, H.; Boer, J.; Deng, H.; Dodd, R.; Essers, M.; Feuerstein, T.; Gallagher, B. M., Jr.; Gege, C.; Hochgürtel, M.; Hofmann, M.; Jaworski, A.; Jin, L.; Kiely, A.; Korniski, B.; Kroth, H.; Nix, D.; Nolte, B.; Piecha, D.; Powers, T. S.; Richter, F.; Schneider, M.; Steeneck, C.; Sucholeiki, I.; Taveras, A.; Timmermann, A.; Veldhuizen, J. V.; Weik, J.; Wu, X.; Xia, B. A new class of potent matrix metalloproteinase 13 inhibitors for potential treatment of osteoarthritis: evidence of histologic and clinical efficacy without musculoskeletal toxicity in rat models. *Arthritis Rheum.* **2009**, *60*, 2008–2018.
- (8) Wojtowicz-Praga, S.; Torri, J.; Johnson, M.; Steen, V.; Marshall, J.; Ness, E.; Dickson, R.; Sale, M.; Rasmussen, H. S.; Chiodo, T. A.; Hawkins, M. J. Phase I trial of marimastat, a novel matrix metalloproteinase inhibitor, administered orally to patients with advanced lung cancer. *J. Clin. Oncol.* **1998**, *16*, 2150–2156.
- (9) Stickens, D.; Behonick, D. J.; Ortega, N.; Heyer, B.; Hartenstein, B.; Yu, Y.; Fosang, A. J.; Schorpp-Kistner, M.; Angel, P.; Werb, Z. Altered endochondral bone development in matrix metalloproteinase 13-deficient mice. *Development* **2004**, *131*, 5883–5895.
- (10) Kennedy, A. M.; Inada, M.; Krane, S. M.; Christie, P. T.; Harding, B.; López-Otín, C.; Sánchez, L. M.; Pannett, A. J.; Dearlove, A.; Hartley, C.; Byrne, M. H.; Reed, A.; Nesbit, M. A.; Whyte, M. P.; Thakker, R. V. MMP13 mutation causes spondyloepimetaphyseal dysplasia, Missouri type (SEMDMO). *J. Clin. Invest.* **2005**, *115*, 2832–2842.
- (11) Engel, C. K.; Pirard, B.; Schimanski, S.; Kirsch, R.; Habermann, J.; Klingler, O.; Schlotte, V.; Weithmann, K. U.; Wendt, K. U. Structural basis for the highly selective inhibition of MMP-13. *Chem. Biol.* **2005**, *12*, 181–189.
- (12) Li, J. J.; Nahra, J.; Johnson, A. R.; Bunker, A.; O'Brien, P.; Yue, W.-S.; Ortwine, D. F.; Man, C.-F.; Baragi, V.; Kilgore, K.; Dyer, R. D.; Han, H.-K. Quinazolinones and pyrido[3,4-d]pyrimidin-4-ones as orally active and specific matrix metalloproteinase-13 inhibitors for the treatment of osteoarthritis. *J. Med. Chem.* **2008**, *51*, 835–841.
- (13) Schnute, M. E.; O'Brien, P. M.; Nahra, J.; Morris, M.; Roark, W. H.; Hanau, C. E.; Ruminski, P. G.; Scholten, J. A.; Fletcher, T. R.; Hamper, B. C.; Carroll, J. N.; Patt, W. C.; Shieh, H. S.; Collins, B.; Pavlovsky, A. G.; Palmquist, K. E.; Aston, K. W.; Hitchcock, J.; Rogers, M. D.; McDonald, J.; Johnson, A. R.; Munie, G. E.; Wittwer, A. J.; Man, C.-F.; Settle, S. L.; Nemirovskiy, O.; Vickery, L. E.; Agawal, A.; Dyer, R. D.; Sunyer, T. Discovery of (pyridin-4-yl)-2H-tetrazole as a novel scaffold to identify highly selective matrix metalloproteinase-13 inhibitors for the treatment of osteoarthritis. *Bioorg. Med. Chem. Lett.* **2010**, *20*, 576–580.
- (14) Nara, H.; Sato, K.; Naito, T.; Mototani, H.; Oki, H.; Yamamoto, Y.; Kuno, H.; Santou, T.; Kanzaki, N.; Terauchi, J.; Uchikawa, O.; Kori, M. Discovery of novel, highly potent, and selective quinazoline-2-carboxamide-based Matrix metalloproteinase (MMP)-13 inhibitors without a zinc binding group using a structure-based design approach. *J. Med. Chem.* **2014**, *57*, 8886–8902.
- (15) Nara, H.; Sato, K.; Naito, T.; Mototani, H.; Oki, H.; Yamamoto, Y.; Kuno, H.; Santou, T.; Kanzaki, N.; Terauchi, J.; Uchikawa, O.; Kori, M. Thieno[2,3-d]pyrimidine-2-carboxamides bearing a carboxybenzene group at 5-position: Highly potent, selective, and orally available MMP-13 inhibitors interacting with the S1' binding site. *Bioorg. Med. Chem.* **2014**, *22*, 5487–5505.
- (16) Gege, C.; Bao, B.; Bluhm, H.; Boer, J.; Gallagher, B. M., Jr.; Korniski, B.; Powers, T. S.; Steeneck, C.; Taveras, A. G.; Baragi, V. M. Discovery and evaluation of a non-Zn chelating, selective matrix metalloproteinase 13 (MMP-13) inhibitor for potential intra-articular treatment of osteoarthritis. *J. Med. Chem.* **2012**, *55*, 709–716.
- (17) Taylor, S. J.; Abeywardane, A.; Liang, S.; Muegge, I.; Padyana, A. K.; Xiong, Z.; Hill-Drzewi, M.; Farmer, B.; Li, X.; Collins, B.; Li, J. X.; Heim-Riether, A.; Proudfoot, J.; Zhang, Q.; Goldberg, D.; Zuvella-Jelaska, L.; Zaher, H.; Li, J.; Farrow, N. A. Fragment-based discovery of indole inhibitors of matrix metalloproteinase-13. *J. Med. Chem.* **2011**, *54*, 8174–8187.
- (18) Cai, H.; Agrawal, A. K.; Putt, D. A.; Hashim, M.; Reddy, A.; Brodfuehrer, J.; Surendran, N.; Lash, L. H. Assessment of the renal toxicity of novel anti-inflammatory compounds using cynomolgus monkey and human kidney cells. *Toxicology* **2009**, *258*, 56–63.
- (19) Sallustio, B. C.; Sabordo, L.; Evans, A. M.; Nation, R. L. Hepatic disposition of electrophilic acyl glucuronide conjugates. *Curr. Drug Metab.* **2000**, *1*, 163–180.
- (20) Summerbell, R. K.; Stephens, J. R. The stereochemistry of several 2,5-disubstituted dioxanes. *J. Am. Chem. Soc.* **1954**, *76*, 6401–6407.
- (21) Obach, R. S. Prediction of human clearance of twenty-nine drugs from hepatic microsomal intrinsic clearance data: An examination of in vitro half-life approach and nonspecific binding to microsomes. *Drug Metab. Dispos.* **1999**, *27*, 1350–1359.
- (22) Stepan, A. F.; Karki, K.; McDonald, W. S.; Dorff, P. H.; Dutra, J. K.; DiRico, K. J.; Won, A.; Subramanyam, C.; Efreimov, I. V.; O'Donnell, C. J.; Nolan, C. E.; Becker, S. L.; Pustilnik, L. R.; Sneed, B.; Sun, H.; Lu,

Y.; Robshaw, A. E.; Riddell, D.; O'Sullivan, T. J.; Sibley, E.; Capetta, S.; Atchison, K.; Hallgren, A. J.; Miller, E.; Wood, A.; Obach, R. S. Metabolism-Directed Design of Oxetane-Containing Arylsulfonamide Derivatives as  $\gamma$ -Secretase Inhibitors. *J. Med. Chem.* **2011**, *54*, 7772–7783.

(23) Ritchie, T. J.; Macdonald, S. J. F.; Peace, S.; Pickett, S. D.; Luscombe, C. N. The developability of heteroaromatic and heteroaliphatic rings – do some have a better pedigree as potential drug molecules than others? *MedChemComm* **2012**, *3*, 1062–1069.

(24) St. Jean, D. J., Jr.; Fotsch, C. Mitigating heterocycle metabolism in drug discovery. *J. Med. Chem.* **2012**, *55*, 6002–6020.

(25) Katz, J. D.; Jewell, J. P.; Guerin, D. J.; Lim, J.; Dinsmore, C. J.; Deshmukh, S. V.; Pan, B.-S.; Marshall, C. G.; Lu, W.; Altman, M. D.; Dahlberg, W. K.; Davis, L.; Falcone, D.; Gabarda, A. E.; Hang, G.; Hatch, H.; Holmes, R.; Kunii, K.; Lumb, K. J.; Lutterbach, B.; Mathvink, R.; Nazef, N.; Patel, S. B.; Qu, X.; Reilly, J. F.; Rickert, K. W.; Rosenstein, C.; Soisson, S. M.; Spencer, K. B.; Szewczak, A. A.; Walker, D.; Wang, W.; Young, J.; Zeng, Q. Discovery of a 5*H*-benzo[4,5]cyclohepta[1,2-*b*]pyridin-5-one (MK-2461) inhibitor of c-Met kinase for the treatment of cancer. *J. Med. Chem.* **2011**, *54*, 4092–4108.

(26) Del Bello, F.; Barocelli, E.; Bertoni, S.; Bonifazi, A.; Camalli, M.; Campi, G.; Giannella, M.; Matucci, R.; Nesi, M.; Pignini, M.; Quaglia, W.; Piergentili, A. 1,4-Dioxane, a suitable scaffold for the development of novel M3 muscarinic receptor antagonists. *J. Med. Chem.* **2012**, *55*, 1783–1787.

(27) Mammoli, V.; Bonifazi, A.; Del Bello, F.; Diamanti, E.; Giannella, M.; Hudson, A. L.; Mattioli, L.; Perfumi, M.; Piergentili, A.; Quaglia, W.; Titomanlio, F.; Pignini, M. Favourable involvement of  $\alpha_{2A}$ -adrenoreceptor antagonism in the I<sub>2</sub>-imidazoline binding sites-mediated morphine analgesia enhancement. *Bioorg. Med. Chem.* **2012**, *20*, 2259–2265.

(28) Settle, S.; Vickery, L.; Nemirovskiy, O.; Vidmar, T.; Bendele, A.; Messing, D.; Ruminski, P.; Schnute, M.; Sunyer, T. Cartilage degradation biomarkers predict efficacy of a novel, highly selective matrix metalloproteinase 13 inhibitor in a dog model of osteoarthritis confirmation by multivariate analysis that modulation of type II collagen and aggrecan degradation peptides parallels pathologic changes. *Arthritis Rheum.* **2010**, *62*, 3006–3015.

(29) Tortorella, M. D.; Tomasselli, A. G.; Mathis, K. J.; Schnute, M. E.; Woodard, S. S.; Munie, G.; Williams, J. M.; Caspers, N.; Wittwer, A. J.; Malfait, A. M.; Shieh, H. S. Structural and inhibition analysis reveals the mechanism of selectivity of a series of aggrecanase inhibitors. *J. Biol. Chem.* **2009**, *284*, 24185–24191.